THE UNIVERSITY OF MICHIGAN

INDUSTRY PROGRAM OF THE COLLEGE OF ENGINEERING

THERMAL LOADING AND WALL TEMPERATURE AS FUNCTIONS OF PERFORMANCE OF TURBOCHARGED COMPRESSION IGNITION ENGINES

E. T. Vincent
N. A. Henein

August, 1958

IP-307

TABLE OF CONTENTS

LIST OF FIGURES

LIST OF FIGURES (CONT'D)

THERMAL LOADING AND WALL TEMPERATURES AS FUNCTIONS OF PERFORMANCE OF TURBOCHARGED COMPRESSION IGNITION ENGINES

INTRODUCTION

The first approach to turbocharging dates back to the early 1900 and some practical applications occurred at that early date. The demand for high duty engines of the compression ignition type has increased enormously since the end of World War II to such an extent that most engine manufacturers now offer models equipped for tubo-charging. This development has resulted due to the following factors:

1. The demand for higher power outputs at maximum fuel economy.
2. The availability of improved heat resisting alloys and technology which has resulted in exhaust gas turbine chargers having the desired degree of reliability and life for the service conditions to be encountered.
3. Improved engine materials, bearings and oils to carry the extra loads, temperatures etc.

The factors which limit the output of the oil engine are many and varied. A partial list would appear as follows:

1. Cycle of operations
2. Combustion system (open chamber, pre-combustion chamber, etc.)
3. Bearing capacities
4. Stress levels
5. Heat disposal
6. Breathing capacity

7. Durability

8. Reliability

It is believed that the most important factors as regards output are three in number viz:

a. Mechanical stressing of parts and bearings

b. Oxygen content of cylinder

c. Internal temperature of working surfaces.

If the above three items are controlled in a satisfactory manner little doubt exists that a successful engine can be built around these items. Little need be said regarding item (a) it is well understood, much work has been published regarding it.

Item (b) the oxygen content of the cylinder determines the amount of fuel that can be burnt per cycle and thus the power output or indicated mean effective pressure. It is here that the reason for turbo-charging is found -- it is a means of increasing the oxygen of the cylinder at little or no expense in burning some of this oxygen to supply the additional charge of oxygen; the energy for supercharging is obtained from the exhaust gases, not from the power output of the cylinders and thus the oxygen supply as in the case with mechanically driven superchargers. This observation is true provided that the application of the turbine in the exhaust stream does not impose power drop of any magnitude on the engine output.

The application of supercharging of itself does not assure increased performance, the combustion process can change for the worse when, little improvement in output or economy is to be expected. Under such conditions, resulting from poor combustion, the combustion extends late into the expansion

stroke producing mainly an increased temperature of the parts and heat loss to the jackets with failure of the lubricating oil film and piston seizure to be expected.

If turbo-charging is applied correctly resulting in improved specific fuel consumption the cylinder pressures and gas density increase, as can also the maximum gas temperature. All these factors also lead to increased heat transmission to the jacket, despite a reduction of the percentage heat loss to the coolant. It follows that the internal surface temperature of the cylinder must also increase, reducing the margin of safety provided by the oil film. It follows that the designer should have means available for the calculation of heat flow problems as well as those for pressure, power output etc.

As a result of a cycle analysis investigation carried out during World War II a method was dveloped whereby the effect of heat transfer on specific fuel consumption and power output could be calculated in a very satisfactory manner for both spark and compression ignition engines[1]. As a further advance in the heat flow problem the authors looked into the possibilities of solving the problem of the actual surface temperature of the engine cylinder in the hope of supplying means of determining this important missing limitation on modern engine output which is not covered at present. Then with the combination of modern stress calculation and measurement accurate cycle pressure and temperature estimation plus working surface temperatures it would be possible to predict all of the major parameters for any proposed engine design.

It is too optimistic to conclude that this present attempt is the final answer to the problem, however, it presents a method by which the internal surface temperatures of cylinder walls can be predicted from a knowledge of the cycle pressure and temperatures when such is available, or by the use of Reference 1, together with the present method it would be possible to examine with some degree of accuracy the stresses, power possibilities and heat limitations of any proposed engine type operating on any type of cycle.

The results presented here show reasonable agreement between the calculated and measured mean surface temperature over a wide range of operation, so much so, that it is believed possible to predict limiting power output due to heat flow if a maximum wall temperature is known or assumed; at least for the type of engine tested.

The material to be presented is divided under three headings as follows:

1. Theory
   a. Theory of heat transfer in an engine cylinder
   b. Theory for the calculation of combustion chamber wall temperature.
2. Experimental Data
   a. Cylinder pressure recording
   b. Instantaneous wall temperature recording
   c. Heat transfer to coolant
   d. Experimental procedure and test results
3. Analysis of Experimental Results
   a. Heat transfer
   b. Calculation of wall temperature

c. Calculation of total thermal load on engine

d. Effects of after cooling

Theory of Heat Transfer in an Engine Cylinder

The heat transfer to the coolant in an engine occurs in three steps:

1. Heat transfer between the gases and the walls.
2. Heat transfer through the walls.
3. Heat transfer from the walls to the cooling medium.

In the following paragraphs the process of heat transfer in each of these steps will be discussed separately.

Heat Transfer Between the Gases and the Walls

The rate of heat transfer between a gas and a surrounding surface is, in general, a function of the surface area, the temperature difference between the gas and the surface, and a coefficient of heat transfer. For any internal combustion engine, these factors change from instant-to- instant throughout the cycle.

The surface exposed to the gases in the cylinder varies from a minimum at top dead center to a maximum at bottom dead center. When the piston is at the top dead center, the surface exposed to the gases consists of that of the combustion chamber plus the piston top. As the piston moves toward the bottom dead center, the cylinder bore is exposed to the gases. The surface area variation follows a curve similar to that of Figure 1. The area during the intake and exhaust strokes includes those portions of the intake and exhaust manifolds enclosed in the cylinder head casting

since these manifold walls transfer heat between the gases and the cooling water during the corresponding strokes.

The temperature of the gases in the cylinder varies widely during the different strokes. At the beginning of the intake stroke, the temperature is that of the clearance gases, but falls rapidly as the fresh air is brought in. It rises during the compression stroke, reaches its maximum at the end of the combustion process, then decreases with expansion and drops rapidly after the exhaust valve opens. There is a small drop in temperature during the exhaust stroke.

It follows that the temperature of the inside surface of the cylinder wall will also fluctuate during the cycle, following the variation of the gas temperature. The wall temperature reaching its maximum at the end of the combustion process, then drops continually during the exhaust and intake strokes, and reaches its minimum during the early part of the compression stroke. Figure 2 shows a picture of the wall temperature variations for the whole cycle of the engine during one of the runs.

The change in the coefficient of heat transfer, during the cycle, follows the variations in the gas temperature and pressure. At any instant of the cycle this coefficient is a function of the instantaneous pressure and temperature of the gas. This function was given by G. Eichelberg as,

$$\alpha_g = 2.1 \sqrt[3]{S}\ \sqrt[2]{P}\ T_g \qquad \frac{\text{K. cal.}}{\text{hr. m}^2\text{. 6.}}$$

where α_g = Instantaneous coefficient of heat transfer

S = Mean piston speed in m/sec

P = Pressure in atmospheres

T_g = Gas temperature in degs. Kelvin

Converting this equation into B. T. Us. and ft-lb units the following is obtained

$$\alpha_g = 0.0564 \sqrt[3]{S} \sqrt[2]{P}\, T_g \quad \frac{\text{B. T. U.}}{\text{hr. - sq. ft. - deg.}} \qquad (1)$$

where S = Mean piston speed in ft per sec

P = Pressure in lbs per sq inch

T_g = Degree Rankine

It follows that the equation for the heat transfer to a wall becomes

$$Q = \int_0^t \alpha_g A_g (T_g - T_{wg})dt \qquad (2)$$

where A_g = Area of wall on gas side

T_{wg} = Temperature of wall on gas side

This equation applies to that portion of the combustion chamber wall continually exposed to the heat from the gases. At the same time heat transfer is occurring to some part of the cylinder wall uncovered by the piston. If it is assumed that T_{wg}; of Equation (2) can be considered constant (its variation as compared with that of the gas temperature is negligable as can be seen by inspection of the test results) then the overall heat transfer can be represented by

$$Q = A_{c.ch.}\ \alpha_m (T_{m.e.} - T_{wg}) \qquad (3)$$

where $A_{c.ch}$ = Total area of combustion chamber walls (including piston crown)

α_m = Mean coefficient of heat transfer from gas to wall over the whole cycle.

$T_{m.e.}$ = Gas mean effective temperature over the whole cycle.

$$= \frac{(\alpha_g T_g)_m}{\alpha_m}$$

Heat Transfer Through the Walls.

The heat reaching the walls of the cylinder passes by conduction through the wall by the following equation:

$$Q = A_m \frac{k_w}{X} (T_{wg} - T_{wc}) \qquad (4)$$

where A_m = Mean area of wall

k_w = Thermal conductivity of metal of wall

X = Thickness of wall

T_{wc} = Wall temperature on coolant side

For the reasons given above T_{wg} and T_{wc} can both be considered constant.

Heat Transfer to Coolant

Heat transfer through the wall is followed by transfer to the coolant which is mainly considered as convective when

$$Q = \alpha_c A_c (T_{wc} - T_c) \qquad (5)$$

where A_c = Area of wall on coolant side

α_c = Coefficient of heat transfer from wall to cooling water

T_c = Cooling water temperature

The value of α_c will be some function of the rate of flow of the cooling medium, its physical properties, and the actual mechanism of cooling. It was assumed that for a water cooled engine α_c can be calculated by using Nusselt's equation

$$\frac{\alpha D}{k} = C_1 \left(\frac{VD\rho}{\mu}\right)^m \left(\frac{c\mu}{k}\right)^n \qquad (6)$$

where D = Constant for a given engine

k = Thermal conductivity of water

V = Velocity of flow

ρ = Density

μ = Dynamic viscosity

c = Specific heat

On the basis that ($V\rho$) is proportional to the rate of flow of the coolant and that k is a constant at the given temperature maintained by the thermostat, then Nusselt's equation becomes

$$\alpha_c = C_1\left(\frac{W_c}{\mu}\right)^m \left(\frac{c\mu}{k}\right)^n \qquad (7)$$

The values of the exponents m and n were given by B. Pinkel[2] as m = 0.6 and n = 0.4 while the constant C_1 is to be determined for each engine.

The heat flow to the wall from the gas, through the wall and to the coolant is of constant magnitude. It follows that by equating and rearranging Equations (3), (4) and (5) Equation (8) is obtained

$$\frac{k_w}{\alpha_m(T_{me} - T_{wg})} = \frac{A_g}{A_m}\left(\frac{X}{T_{wg} - T_{wc}}\right) = \frac{A_g}{A_c}\left(\frac{k_w}{\alpha_c\ (T_{wc} - T_c)}\right) \qquad (8)$$

Combustion Chamber Wall Temperature

Examination of Equation (8) shows that if an imaginary thickness $\left(\frac{k_w}{\alpha_M}\right)$, be placed on the gas side of the combustion chamber wall and another one of thickness $\left(\frac{k_w}{\alpha_c}\right)\left(\frac{A_g}{A_c}\right)$ on the colling side with the conductivity of these imaginary walls equal to that of the chamber wall, then a straight

line between the mean effective temperature of the gas and cooling water temperature, will intersect the wall at a temperature equal to that of the wall as shown in Figure 3. The equation for this temperature is

$$T_{w.g.} = T_{M.E.}\left(\frac{Z}{Z + \frac{k_w}{\alpha_M}}\right) + T_c\left(\frac{\frac{k_w}{\alpha_M}}{\frac{k_w}{\alpha_M} + Z}\right) \qquad (9)$$

where

$$Z = \frac{A_g}{A_m} x + \frac{A_g}{A_c} \cdot \frac{k_w}{\alpha_c}$$

While the thermal load on the cylinder walls is given by the amount of heat transfer to the wall per unit time. viz:

$$Q = A_M U (T_{M.E.} - T_c)$$

where A_M = The mean effective area of heat transfer

U = The overall coefficient of heat transfer between the gases and the cooling medium. U can be calculated from the following equation:

$$\frac{1}{U} = \frac{1}{\alpha_m} + \frac{A_g}{A_m} \cdot \frac{X}{k_w} + \frac{A_g}{A_c} \cdot \frac{1}{\alpha_c} \qquad (10)$$

Similar equations were set up for the piston heat flow and temperature.

Experimental Apparatus

A single cylinder, 4-stroke cycle, liquid-cooled Nordberg Diesel engine was used in the experimental work. The cylinder had a bore of four and a half inches, a stroke of five and a quarter inches and a compression ratio of 14.5. The general test setup is shown in Figures 4 and 5.

The air intake system is shown schematically in Figure 6. Air under pressure entered the system through a filter to eliminate entrained

solids and then passed through an automatic pressure regulating valve before entering the flow meter. This consisted of an A.S.M.E. sharp edged orifice in a flange mounting. Air leaving the flow meter passed through an electric heater to be raised to the required temperature. The heater had a capacity of 3000 watts, with three coils connected in parallel through a switch which allowed reduced power outputs of 1500 or 750 watts. A copper-wool chamber and a surge tank were placed between the heater and the engine intake manifold, to reduce pulsation to a minimum. The surge tank had a capacity of 40.5 times the engine swept volume.

On the exhaust side of the engine a surge tank was connected between the engine and the main conduit. The discharge pipe from the surge tank had a 2-inch gate valve to throttle the exhaust gas flow thus building the required back pressure.

The cooling water system was of the closed type, equipped with a heat exchanger. It consisted of a pump driven by the engine, the heat exchanger, an automatic thermostatic control with a manual temperature control and a water flow meter. The manual control was set to keep the water temperature at about 160°F as it entered the engine.

The fuel weighing system measured the time required for the engine to consume definite weights of fuel. The system, consisted of a scale which was equipped with a mercoid contactor. This operated electrical circuits which started and stopped an elapsed-time electric clock, and a revolution counter. The scale, clock and counter measured the time required for the engine to consume a predetermined weight of fuel, and the number of revolutions of the crankshaft during the same period of time.

A D.C. electric dynamometer of the cradle type was used to start the engine and absorb the power developed and measure the brake output.

THE GAS PRESSURE INDICATOR

This consisted of a pressure pick-up unit and a crank-degree marking unit. The pick-up unit was of the two catenary shaped diaphragm type. Its function was to convert the cylinder pressure variations into corresponding voltage variations which were amplified and fed to a channel of a dual beam oscilloscope.

The degree marks were produced by a steel disc 20 inches diameter, 1/8" thick, mounted on the engine flywheel. The rim of the disc was slotted at three degrees intervals, with deeper slots at 45 degrees intervals. A magnetic pick-up was mounted on the flywheel casing, with its pole close to the rim. The current generated by the rotation of the disc was applied to the other channel of the dual-beam oscilloscope used for the pressure measurements. The corresponding figure obtained on the screen consisted of a serrated line across the horizontal diameter of the screen. Every three and forty-five degrees were thereby marked, and one of the deep forty-five degree slots in the disc was alligned at the top dead-center, then the crank angle positions along the indicator diagrma were directly determined. The traces of the gas pressure and crank angles were photographed simultaneously by a polaroid camera.

Combustion Chamber Thermocouple

To measure the rapid temperature changes of the combustion chamber inside-surface, a special Nickel-Steel thermocouple, manufactured by the "Detroit Controls Corporation", was used. As shown in Figure 7, it consists of a "Tyni-couple" basic unit, "Tyni-couple" mount, receptacle plug, and

coaxial cable. The basic unit was mounted with its tip flush with the inside surface of the combustion chamber. The thermocouple junction was at a distance of 0.00025 inch from the tip. Figure 8 shows the details of the thermocouple as it is mounted in the combustion chamber. The position of the thermocouple was chosen in a part of the wall where the above mentioned heat transfer analysis and the resultant equations could be applied.

Shielded copper wires were used to carry the signal to a bridge-amplifier, and a cathode ray oscilloscope. The layout of the temperature recording system being used in the tests is shown in Figure 9. The oscilloscope trace together with the crank angles were photographed simultaneously with a polaroid carera. The reference junction of the thermocouple circuit was at the ambient temperature, which was measured for each test. A sample of the puctures taken for the change in the wall temperature is shown at the top of Figure 2. The lower trace in the same figure is the crank-angle marks.

The theoretical response time, as given by the manufacturer, (Time to reach 62.3% of the imposed surface step change) = 4.5 microseconds. This time is quite short as it is equal to the time required for the crank-shaft to rotate 0.034 of a crank angle at an engine speed of 1200 R.P.M.

Experimental Procedure and Results

The tests covered fuel-air ratios from 0.0134 to 0.055, air manifold pressures up to 45" mercury, air manifold temperatures up to 204° F and engine speeds from 560 to 1770 revolutions per minute. The experiments included two series of tests, each of them with one variable changed at a time. The first series of runs was at variable manifold pressure; the manifold temperature and engine speed were kept constant. The second series of

tests was at variable manifold temperatures at another engine speed.

Since the engine was designed to run under natural aspiration conditions, to avoid troubles due to overloading by supercharging, the following limits were observed. The exhaust temperature not to exceed 1000°F and the gas peak pressure in the cylinder not to exceed 1200 psia. The engine at the end of the tests was in a satisfactory condition, without any sign of failure in any of its parts.

For each test the data necessary for the calculation of the brake output, fuel consumption, air consumption, cooling water losses, wall temperatures at the different points in the engine, and the gas pressure inside the cylinder were taken. Pictures for the following traces were also taken:

a) Gas pressure and crank angles for the whole cycle, a sample is shown in Figure 10 a.

b) Gas pressure and crank angles for the compression and expansion strokes, Figure 10b.

c) Combustion chamber wall temperature and crank angles for the whole cycle, Figure 2a.

d) Combustion chamber wall temperature and crank angles for the combustion period only, Figure 2b.

Some of the interesting experimental results is shown in form of graphs in the figures included in this article. The following is some of the conclusions reached from the experimental results:

1. The measured instantaneous change in the temperature of the inside surface of the wall of the combustion chamber is very small compared to the change in the temperature of the gas.

For the picture shown in Figure 2, this change is 49°F while the change in the gas temperature is 2167°F.

2. The indicated power output of the engine at a constant fuel-air ratio changes in direct proportion with the intake air pressure and inversely with its absolute temperature. When the results shown in Figure 11 were reduced to the same pressure and temperature they resulted in one curve shown in Figure 12.

3. The heat losses change in direct proportion to the indicated mean effective pressure at constant engine speed and intake air temperature. Figure 13 shows the heat losses measured for runs at variable manifold pressures but at constant engine speed and manifold temperature.

4. At constant indicated mean effective pressure and engine speed, the heat losses change in direct proportion to the intake air temperature.

5. The colling losses change in proportion to the cube root of the mean piston speed, with the other conditions kept constant. Figure 14 is for runs at 1200 RPM and 36" mercury with air temperatures ranging from 80°F to 200°F. These curves and other results were reduced to an engine speed of 800 RPM and air temperature of 80°F, and plotted in Figure 15. The curve in the same figure is for another series of tests at the same reduced conditiions, it is the curve of Figure 14.

HEAT-TRANSFER ANALYSIS OF THE EXPERIMENTAL RESULTS

The purpose of this analysis is to calculate the combustion-chamber-wall inside-surface temperature and the thermal load on the cylinder walls, and to check the calculated values with those measured. Equations (9) and (10) will be used for the calculations after finding a relation between, both the mean effective gas temperature and the mean coefficient of heat transfer, and the running conditions of the engine. The running conditions include the manifold temperature, the manifold pressure, the mean piston speed and the indicated mean effective pressure.

The mean effective gas temperature ($T_{M.E.}$), and the gas mean coefficient of heat transfer (α_M) were calculated for each run. For the calculations, the temperature along the cycle was evaluated from the measured gas pressure and the measured air and fuel consumption. This enabled the coefficient of heat transfer (α_g), to be calculated from Equation (1), for the whole cycle as shown in Figure 16. The mean value of α_g was then calculated from the same figure by integration. The mean effective gas temperature could then be calculated by integration of the $\alpha_g T_g$ curve over the whole cycle and Equation (4) see Figure 17.

The mean coefficient of heat transfer and the mean effective gas temperature were then correlated to the mean piston speed, the manifold pressure and temperature. The best correlation of the results was found to give the following relation,

$$T_{M.E.} = \frac{T_m}{\sqrt[3]{P_m \cdot T_m}} \quad \frac{[14.71 + 0.233\ (I.M.E.P.)]}{[\ 0.48 + 0.00157(I.M.E.P.)\ ]} \qquad (11)$$

$$\alpha_M = \sqrt[3]{S}\ \sqrt[3]{P_m \cdot T_m}\ [0.48 + 0.00157\ (I.M.E.P.)] \qquad (12)$$

The constant "C", of Equation (7) for the coefficient of heat transfer from the walls to the cooling water was found experimentally to be equal to 3.15.

Calculation of the Combustion Chamber Wall Temperature

This temperature could be calculated for each run from the above equations and the values for the air manifold pressure, air manifold temperature, engine speed, indicated mean effective pressure, rate of flow of cooling water, temperature of cooling water and other constants for the engine. The mean effective gas temperature, calculated from Equation (11), and the mean coefficient of heat transfer, calculated from Equation (12), were substituted in Equation (9) to get the wall temperature.

When the calculated values of the wall temperature ($T_{w.g.}$) were compared with the values measured by the thermocouple, they were found to be in good agreement. The maximum error was 12.7% with an average of about 4%. Some of this deviation of the measured temperature from that calculated was thought to be due to the following experimental errors:

a) The wall-temperature and the cooling water temperature were not measured simultaneously and a change in the water temperature might have taken place between the two readings. The change in the water temperature could not be held less than $\pm$ 5°F during the run, a result of the thermostatic control being not very sensitive.

b) The indicated mean effective pressure used to calculate the wall temperature was evaluated by adding the friction load measured at the end of the day's tests to the load for the run. The friction load, being a function of the lubricating

oil temperature, was not exactly constant for all the runs of the day, with the result that small errors exist in the indicated mean effective pressure.

c) The average cooling water temperature, used in the calculations, would be lower than the water temperature near the combustion chamber wall, resulting in the majority of the calculated wall temperatures being lower than those measured by the thermocouple.

Calculation of the Thermal Load on the Engine

The thermal load on the cylinder walls was also calculated, and compared with the measured heat losses. As was to be expected, the calculated thermal loads were in general lower than the measured cooling water heat losses. Attention is called to the fact that thethermal load as defined in this paper is not the same as the heat rejected to the coolant, since the latter includes the friction heat. The following equation gives the relation between these heat flows:

$$\text{Thermal load} + \text{Friction heat} = \underset{\text{losses}}{\text{cooling water}} + \underset{\text{outside surface}}{\text{Heat lost from engine}}$$

Again it is pointed out that the friction heat to be accounted for is not equal to the motoring work. In these investigations the friction heat was calculated by extrapolating the cooling losses curve to zero indicated mean effective pressure as shown in Figure 13. This amounted to 3750 BTU/Hr., while the motoring work for the same series of runs was in the range of 6500 BTU/hr.

The difference between the cooling water losses and the thermal load as indicated from the above equation equals the difference between the friction heat and heat lost from the external surfaces of the engine. From Figure 18 this difference amounts to 1250 BTU/Hr., from which the heat lost from the engine outside surface was found equal to 2500 BTU/Hr. This value was thought to be reasonable for the engine used in the tests.

Another way to check the derived equations was to reduce the heat losses to the coolingwater, to the same conditions of manifold and engine speed. From the previous equations the thermal load is proportional to:

$$Q \propto (\alpha_M \cdot T_{M.E.} - \alpha_M \cdot T_{w.g.})$$

Since $T_{w.g.}$ is small compared to $T_{M.E.}$ and the change in the wall temperature is negligible compared to that of the mean effective gas temperature, the thermal load could be considered proportional to $\alpha_M T_{M.E.}$ or in terms of the other variables

$$Q \propto \sqrt[3]{S}\, T_m\, (14.71 + 0.233\ I.M.E.P.)$$

It can be seen then that Q changes in direct proportion to the cube root of the mean piston speed and the manifold absolute temperature. These conclusions agree fairly well with the experimental results mentioned before.

Investigation on Effect of Aftercooling

An investigation was made to find the effect of aftercooling on the engine operation. The arrangement on which calculations were based is shown diagrammatically in Figure 19 . The conditions of operation assumed were as follows:

Compressor efficiency	=	0.80
Atmospheric pressure	=	30" Hg.
Atmospheric temperature	=	80°F
Drop in pressure between compressor and engine manifold	=	0.5 psi.

The calculations were made for three aftercooler effectiveness 0%, 50% and 100%. Other details and method of calculation are given in the original thesis.

The results of the above calculations are shown in Figures 20, 21 and 22. To illustrate more clearly the effect of aftercooling, Figures 23, 24 and 25 were drawn.

The effect of aftercooling on the output (M.E.P.) is shown in Figure 24. It is interesting to notice that the same mean effective pressure could be obtained by supercharging to 45" Hg. without aftercooling, or by supercharging to 41.2" Hg. with an aftercooler affectiveness of 50%. This means that, it would be better, in the interest of lowering the thermal load, to use an aftercooler with an effectiveness 50%, which might result in an additional pressure drop up to 3.8" Hg., rather than to exclude the cooler and keep the pressure at 45" Hg.

The effect of aftercooling on the thermal load is indicated by plotting the intensity of the thermal load vs. the manifold pressure for different effectiveness, (Figure 23). Supercharging at effectiveness 100% has a reducing effect on the thermal load, while supercharging without aftercooling increases the thermal load under the conditions of test. The increase in the air temperature, is seen to have a much greater effect on

increasing the thermal load than the reducing effect of the increased air pressure. An increase of 87°F due to turbocharging to 45" Hg. caused an increase of 22.3% in the thermal load.

It is worthwhile to point out here that, for a mean effective pressure of 140, and a speed of 800 RPM, the thermal load on the cooling system, is reduced by an amount twice as much as the heat removed from the air in the aftercooler. This is illustrated in Figure 25.

The effect of aftercooling on the piston maximum temperature is shown in Figure 23 and 25, which indicate that the temperature drops with aftercooling. A drop of 140°F is a result of aftercooling with effectiveness 50% at a mean effective pressure of 140 and 800 RPM.

CONCLUSIONS

It was concluded that:

1) The thermal load and wall temperature of a turbocharged compression ignition engine are primarily related to the indicated power output and affected to a lesser degree by intake manifold conditions and the engine speed. Results of this investigation show that:

a. The thermal load and wall temperature increase in direct proportion to the indicated mean effective pressure.

b. For the same indicated mean effective pressure:

- Boosting the intake manifold pressure without a corresponding heating of the air will reduce the thermal load and wall temperatures.
- Raising the intake air temperature will increase the thermal load and wall temperature.

- Thermal load changes in direct proportion to the cube root of the mean piston speed.

c. For the same intake manifold pressure the wall temperature changes in direct proportion to the thermal loading.

2) For the operation of turbocharged engines at constant power output and no aftercooling, one of the following two conditions prevails:

a. High supercharging resulting in better fuel economy.

b. Low supercharging resulting in poor fuel economy, but reduced thermal and mechanical loads, without any reduction in the mean wall temperatures.

3) The turbocharged engine performance is improved by increasing the air density and reducing its temperature in the intake manifold resulting in higher specific power outputs and lower thermal loads and wall temperatures. Aftercooling is one method used to increase air density by decreasing the air temperature. Even though the pressure drop increases as the aftercooler effectiveness increases, general engine performance will be improved by using an aftercooler with high effectiveness.

It should be added here that the above investigation was done on one type of combustion chamber. It is believed that similar types of engines will give similar results. But for other types of engines a similar investigation might be needed before using the derived formulae.

REFERENCES

1. Supercharging the Internal Combustion Engine, by E. T. Vincent, McGraw-Hill Book Company.

2. Heat Transfer Processes in Liquid-Cooled Engine Cylinders, by B. Pinkel, E.G. Mangancello and E. Bernardo. NACA, ARRNOE5 g31, 1955.

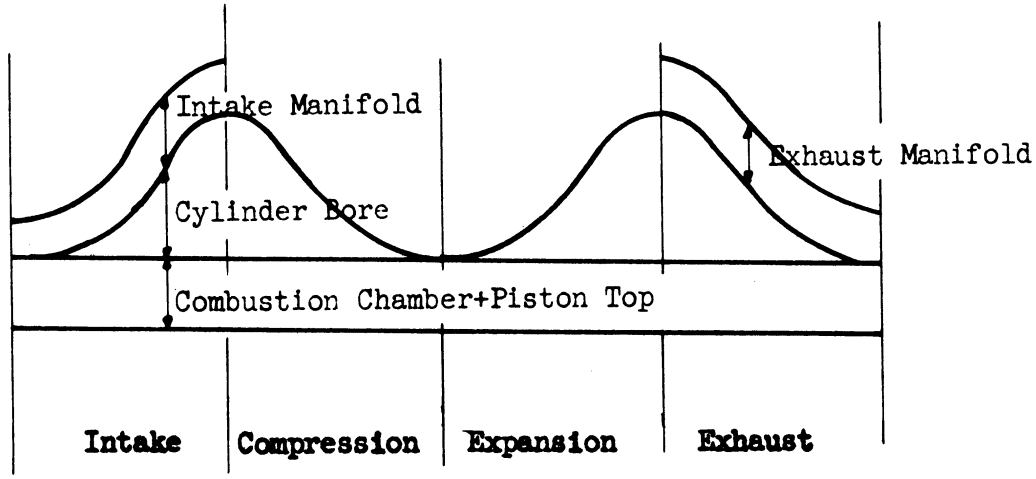

Figure 1. Area of Heat Transfer.

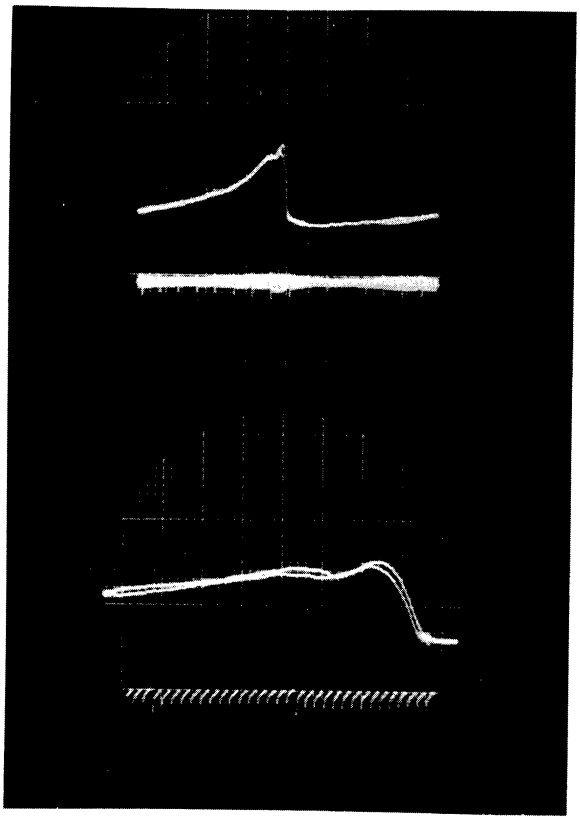

A. Wall temperature and crank angles over the whole cycle (with 3 amplifiers)

B. Wall temperature and cramk angles for the combustion period (with 3 amplifiers)

Figure 2. Combustion Chamber Surface Transient-Temperature.

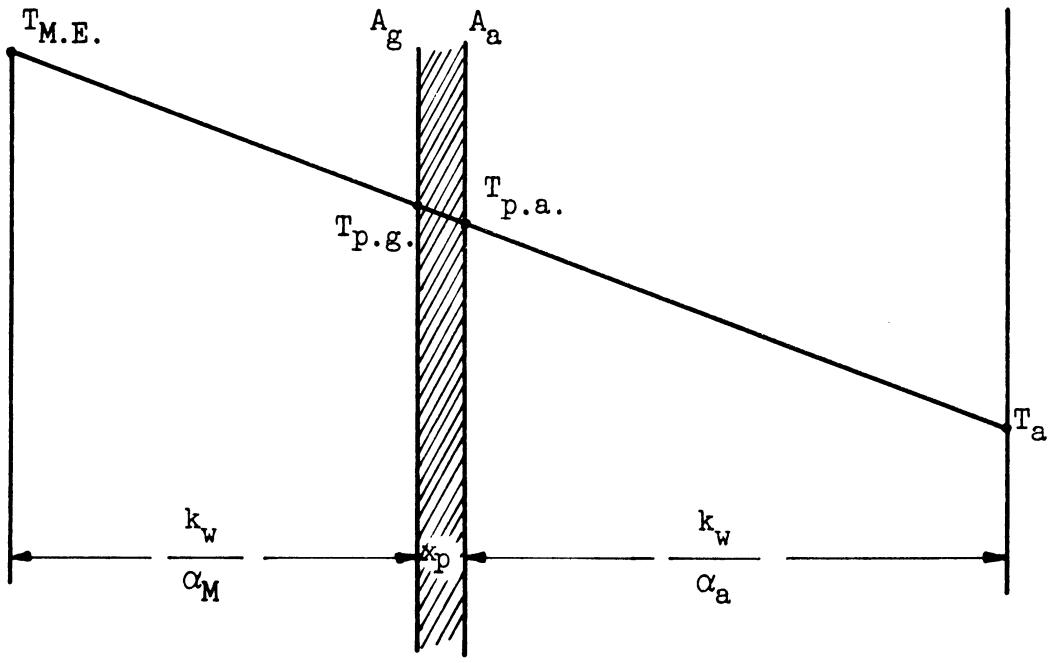

Figure 3. Graphical Construction of the Imaginary Walls for the Piston Crown.

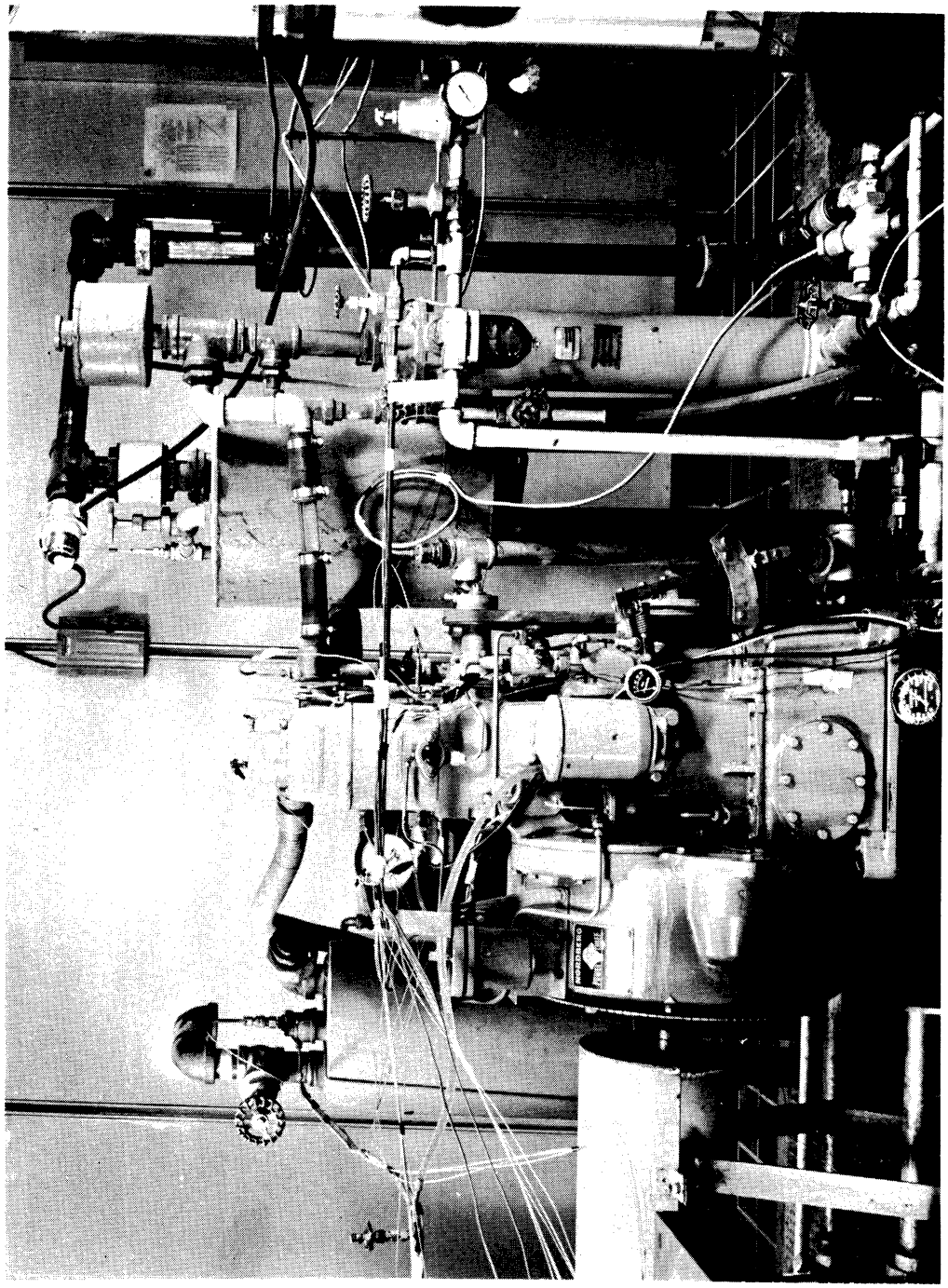

Figure 4. General Layout of the Experimental Setup.

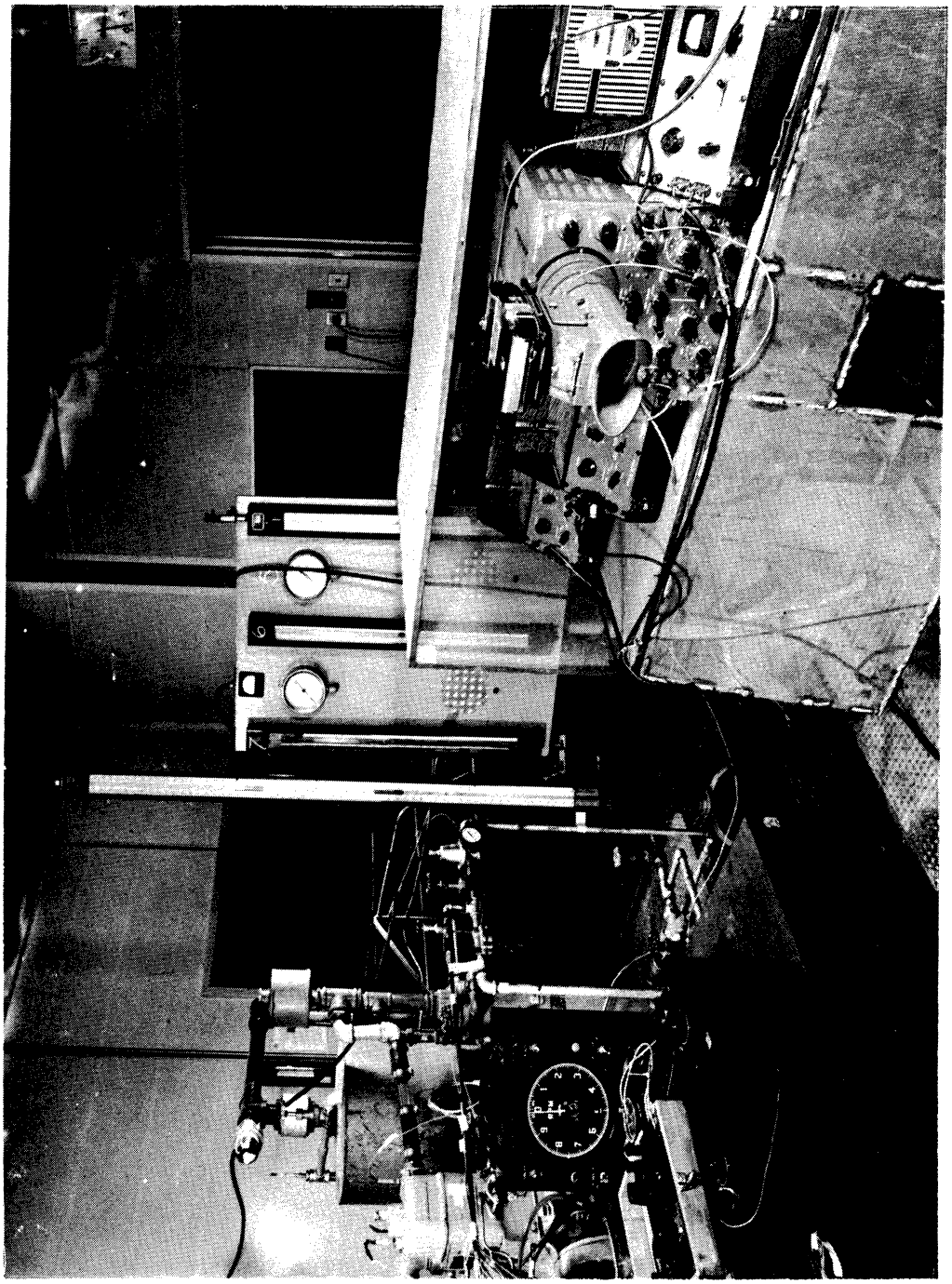

Figure 5. General View of the Oscilloscope and Amplifiers.

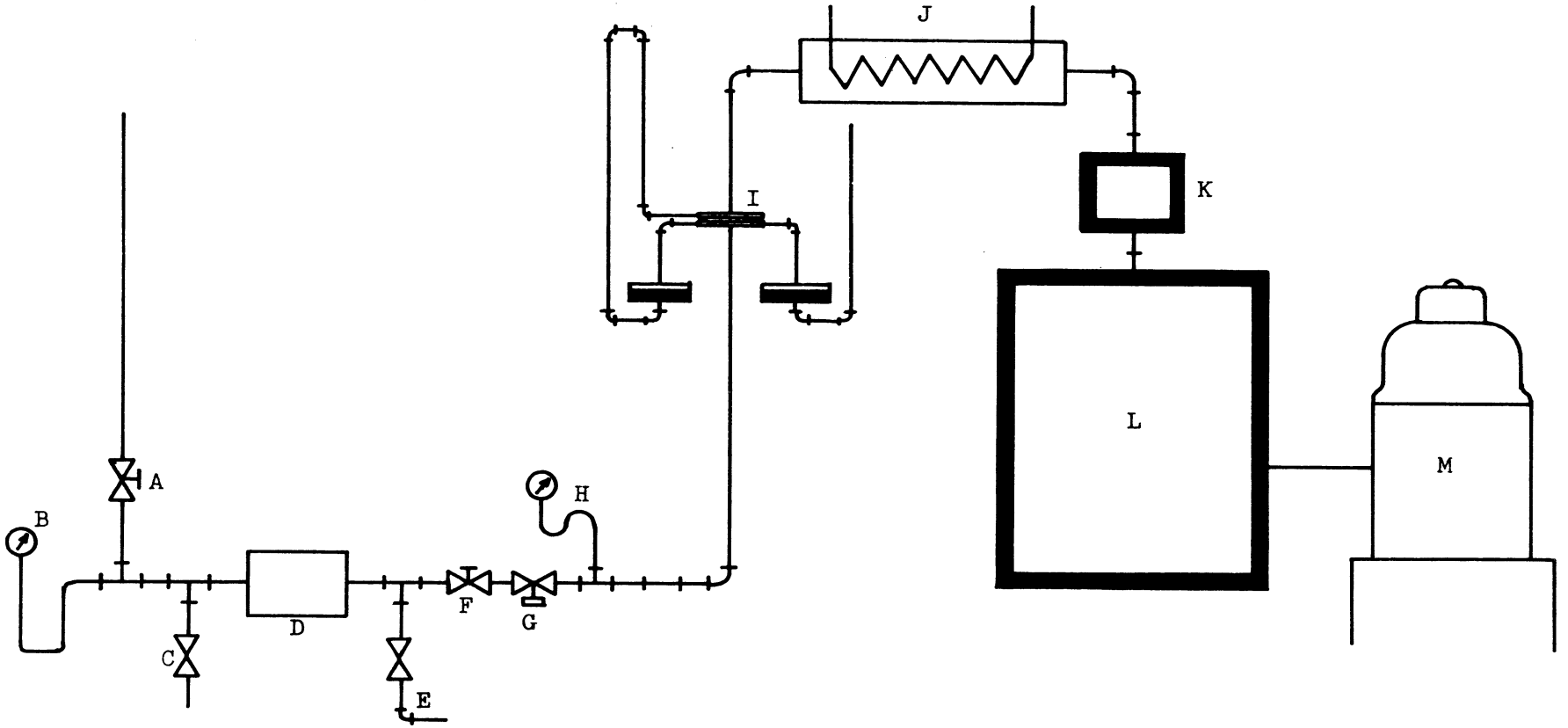

A. Main Air Supply Valve

B. Main Air Pressure Gage

C. Condensate Bleed Valve

D. Air Filter

E. Air Line to Pressure Pick Up

F. Air Supply Valve

G. Air Supply Control Valve

H. Air Pressure Gage

I. Air Flowmeter and Manometers

J. Electric Heater

K. Copper-Wool Chamber

L. Surge Tank

M. Engine

Figure 6. Diagram of Intake System.

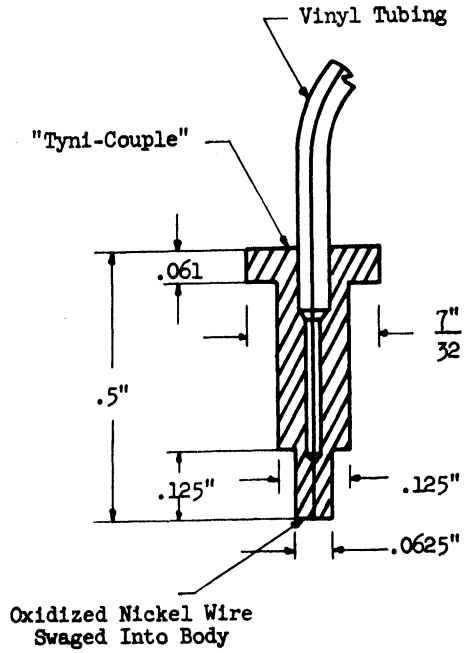

Figure 7a. The Basic "Tyni-Couple" Unit.

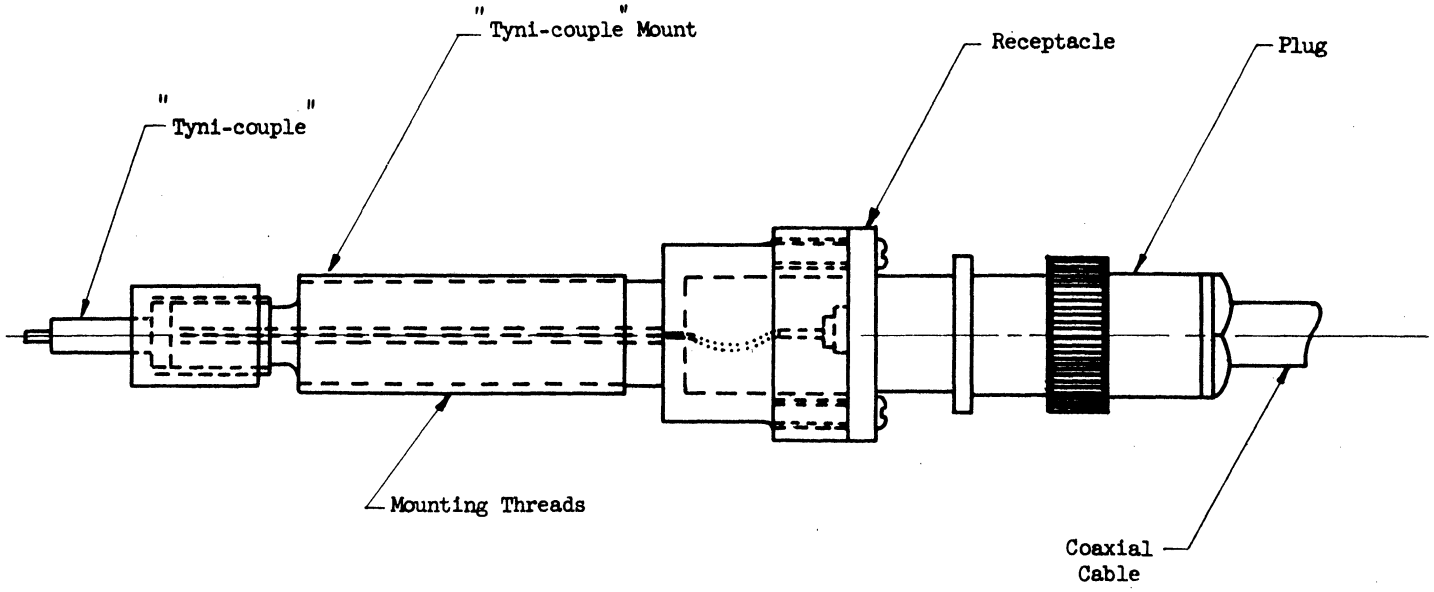

Figure 7b. "Tyni-Couple" Assembly.

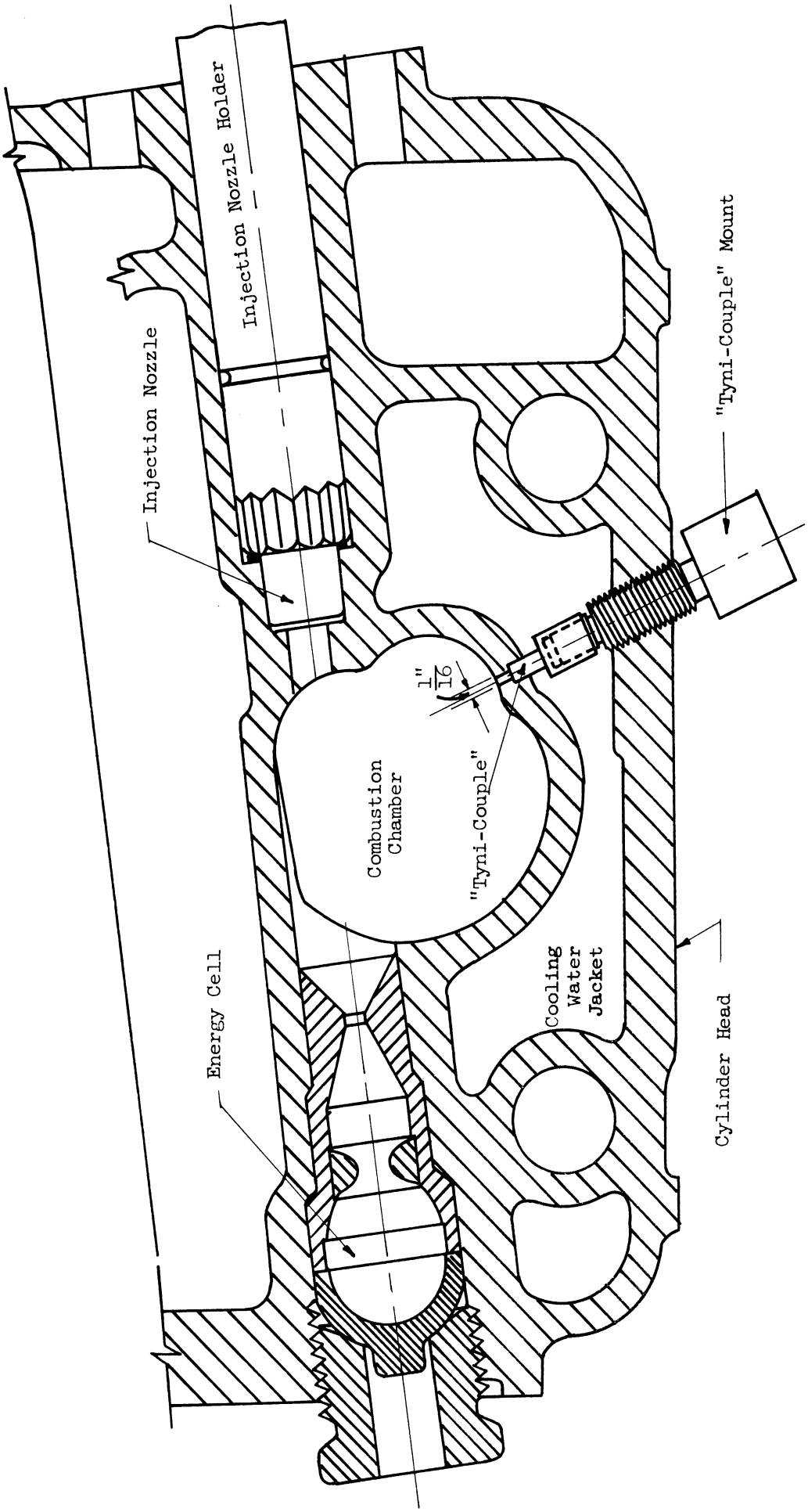

Figure 8. Sectional Plan of Cylinder Head Showing the Combustion-Chamber Thermocouple.

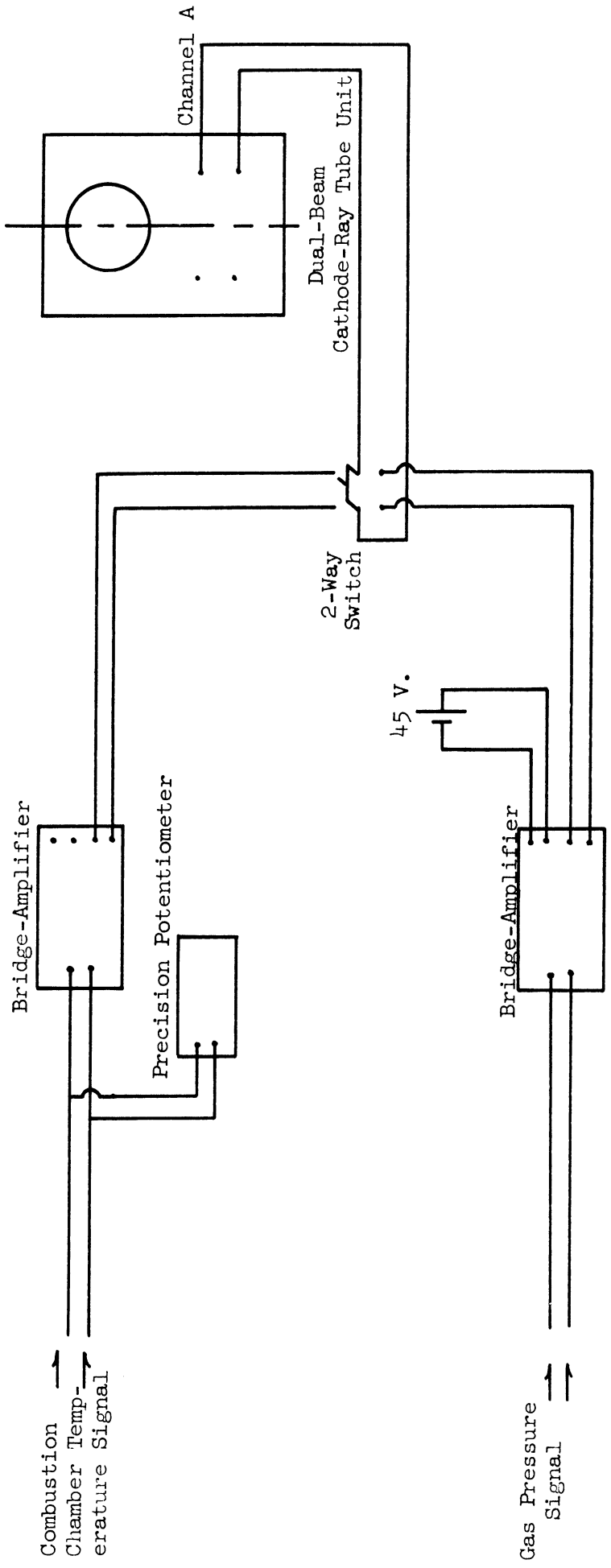

Figure 9. Layout of Electrical Circuits for Pressure and Temperature Recording.

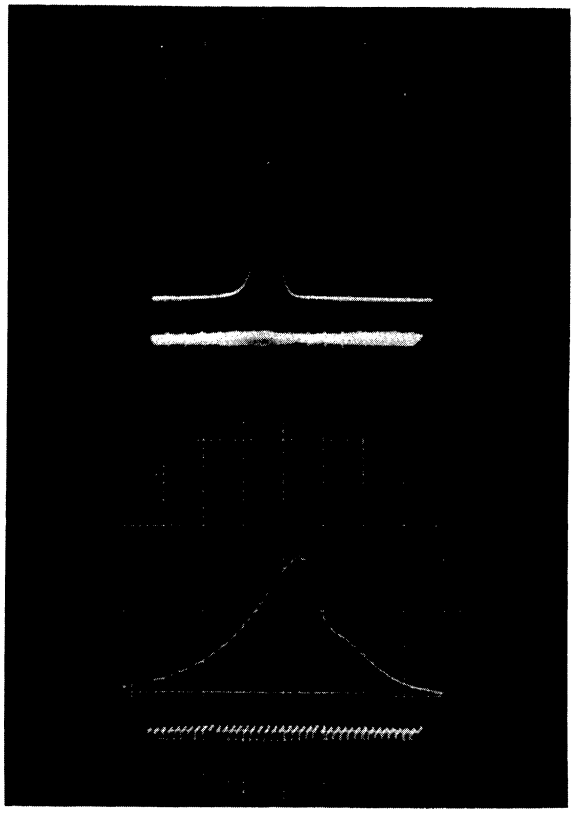

A. Gas pressure and crank angles for the whole cycle.

B. Gas pressure and crank angles for the compression and expansion strokes.

Figure 10. Gas Pressure During the Cycle.

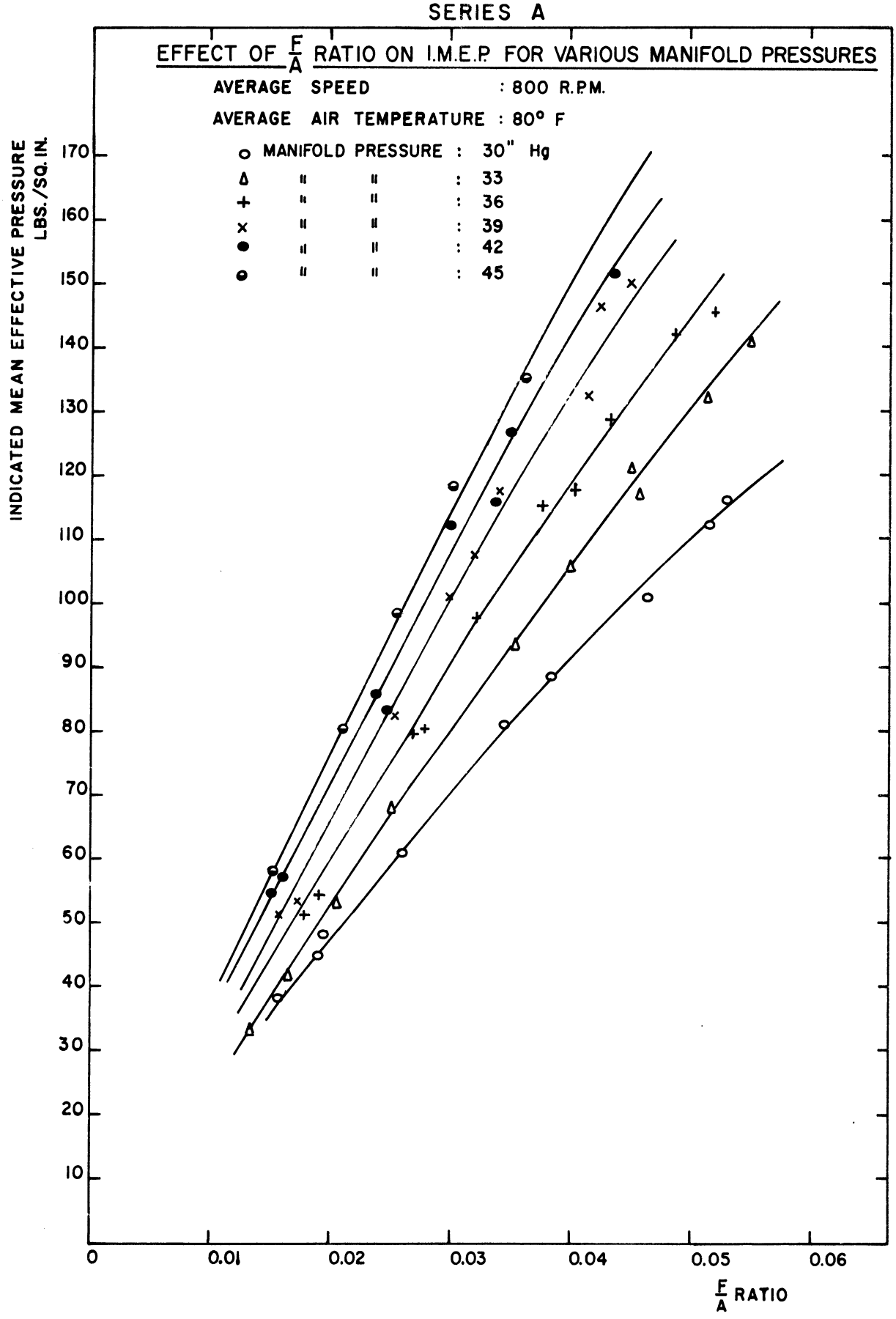
SERIES A
EFFECT OF F/A RATIO ON I.M.E.P FOR VARIOUS MANIFOLD PRESSURES
AVERAGE SPEED : 800 R.P.M.
AVERAGE AIR TEMPERATURE : 80° F
MANIFOLD PRESSURE : 30" Hg
" " : 33
" " : 36
" " : 39
" " : 42
" " : 45
INDICATED MEAN EFFECTIVE PRESSURE LBS./SQ.IN.
170
160
150
140
130
120
110
100
90
80
70
60
50
40
30
20
10
0
0.01
0.02
0.03
0.04
0.05
0.06
F/A RATIO

Figure 11.

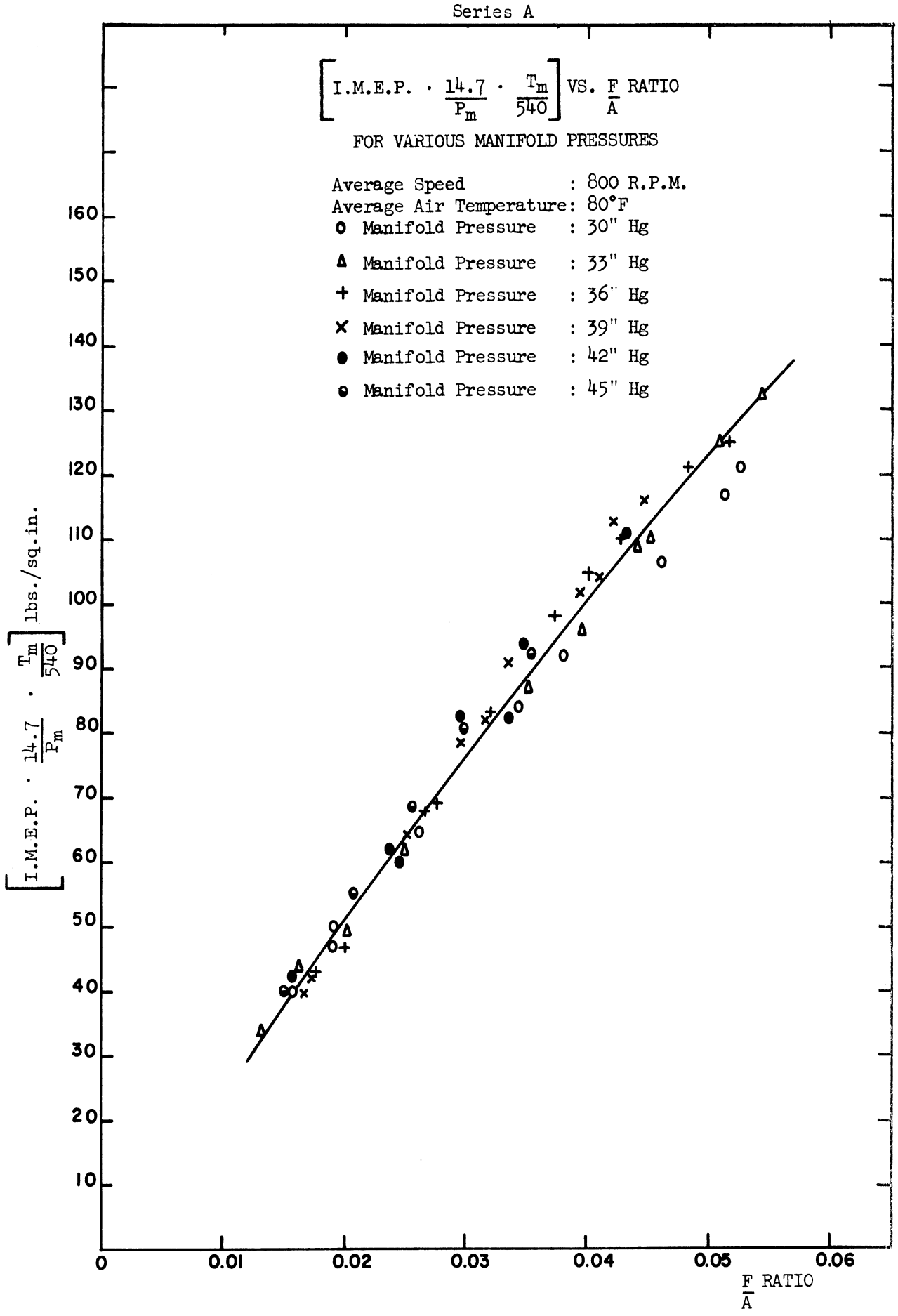
Series A
[I.M.E.P. · 14.7/Pm · Tm/540] VS. F/A RATIO
FOR VARIOUS MANIFOLD PRESSURES
Average Speed : 800 R.P.M.
Average Air Temperature: 80°F
o Manifold Pressure : 30" Hg
Δ Manifold Pressure : 33" Hg
+ Manifold Pressure : 36" Hg
× Manifold Pressure : 39" Hg
● Manifold Pressure : 42" Hg
⊖ Manifold Pressure : 45" Hg
[I.M.E.P. · 14.7/Pm · Tm/540] lbs./sq.in.
160
150
140
130
120
110
100
90
80
70
60
50
40
30
20
10
0
0.01
0.02
0.03
0.04
0.05
0.06
F/A RATIO

Figure 12.

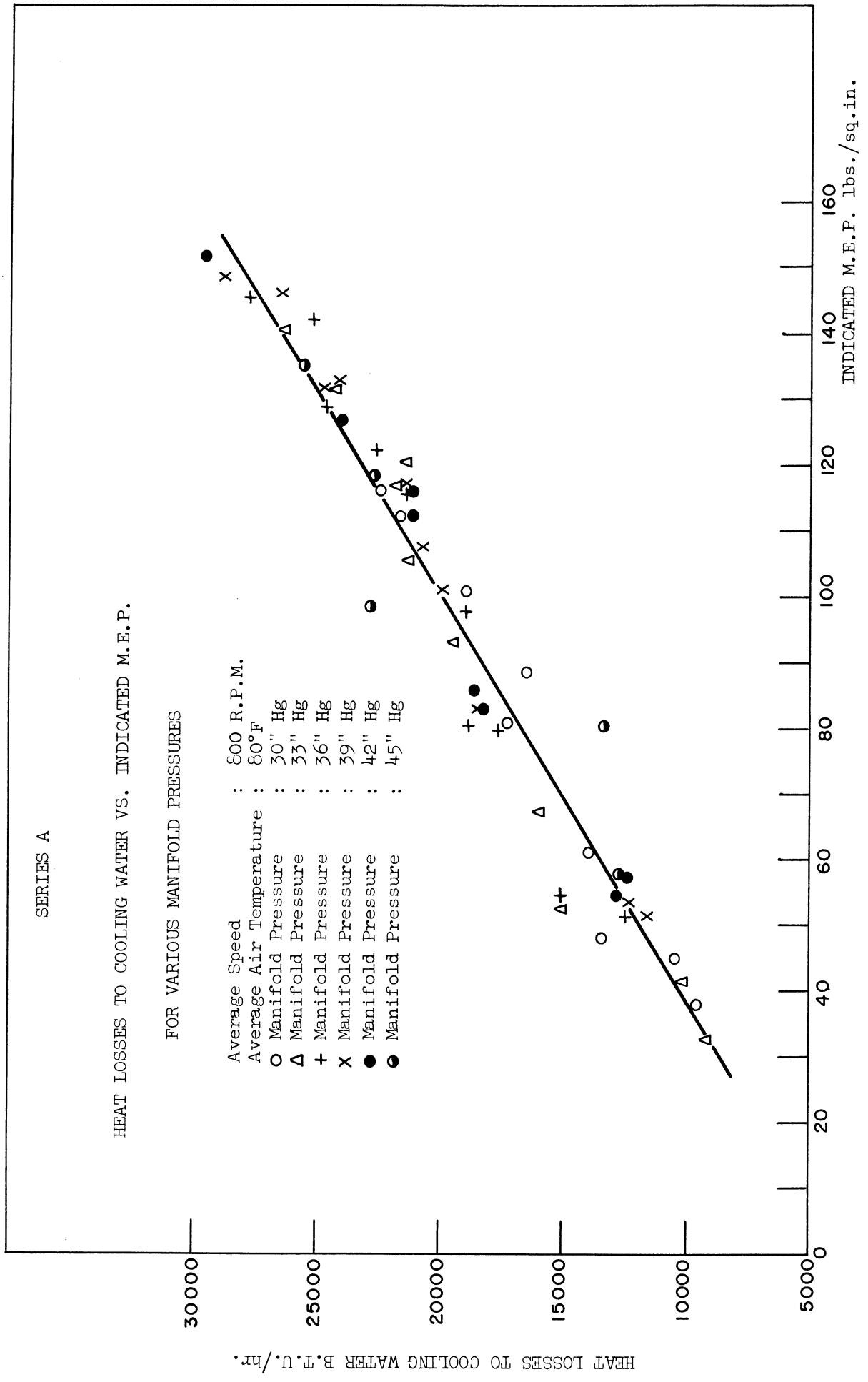
SERIES A
HEAT LOSSES TO COOLING WATER VS. INDICATED M.E.P.
FOR VARIOUS MANIFOLD PRESSURES
Average Speed : 600 R.P.M.
Average Air Temperature : 80°F
O Manifold Pressure : 30" Hg
Δ Manifold Pressure : 33" Hg
+ Manifold Pressure : 36" Hg
× Manifold Pressure : 39" Hg
● Manifold Pressure : 42" Hg
◑ Manifold Pressure : 45" Hg
HEAT LOSSES TO COOLING WATER B.T.U./hr.
30000
25000
20000
15000
10000
5000
0
20
40
60
80
100
120
140
160
INDICATED M.E.P. lbs./sq.in.

Figure 13.

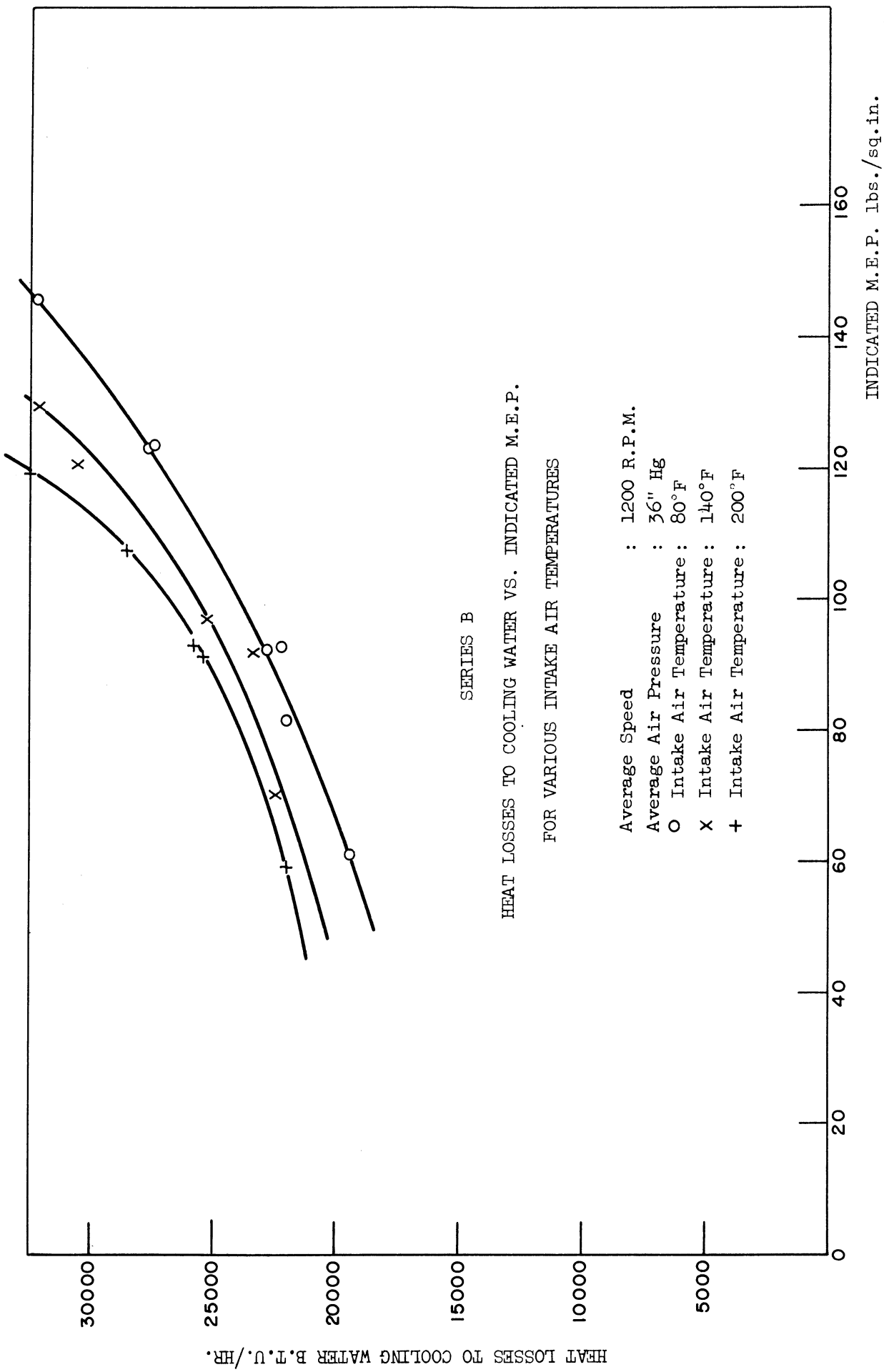
HEAT LOSSES TO COOLING WATER B.T.U./HR.
30000
25000
20000
15000
10000
5000
0
20
40
60
80
100
120
140
160
INDICATED M.E.P. lbs./sq.in.
SERIES B
HEAT LOSSES TO COOLING WATER VS. INDICATED M.E.P.
FOR VARIOUS INTAKE AIR TEMPERATURES
Average Speed : 1200 R.P.M.
Average Air Pressure : 36" Hg
O Intake Air Temperature : 80°F
X Intake Air Temperature : 140°F
+ Intake Air Temperature : 200°F

Figure 14.

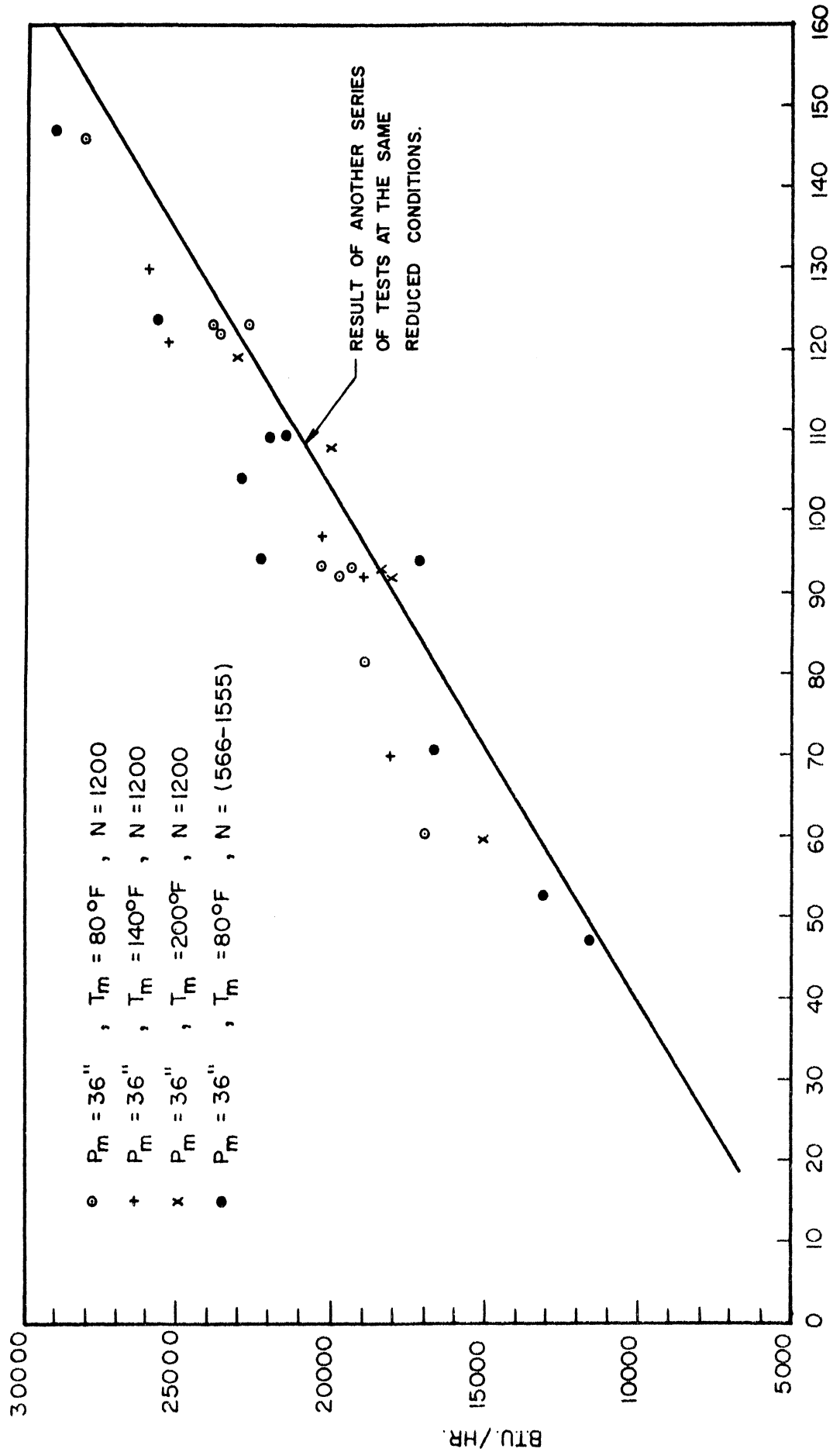

Figure 15. Heat Losses to Cooling Water Reduced to the Same Speed and Intake Air Temperature (N = 800, Tm = 80 F).

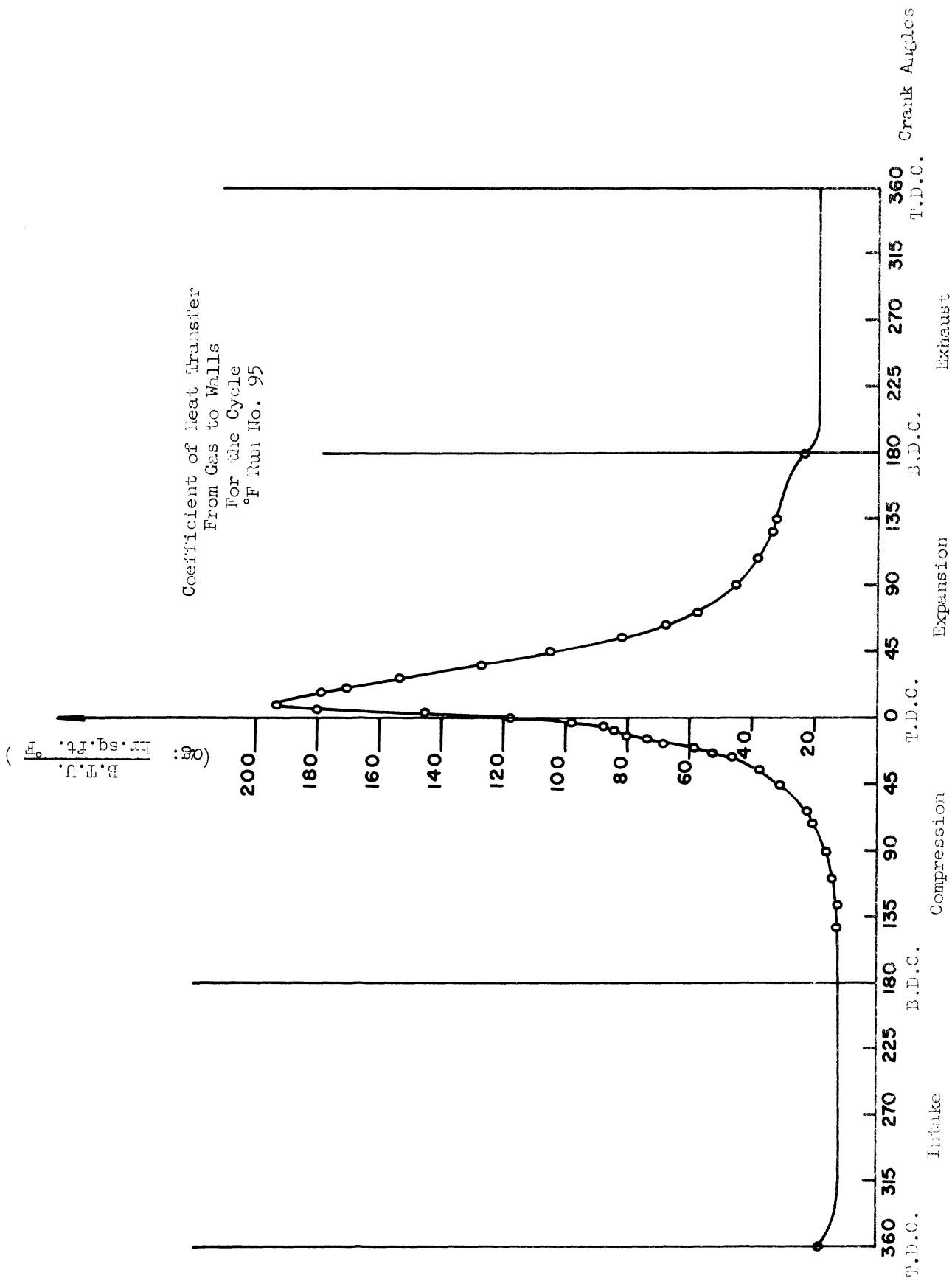
Coefficient of Heat Transfer
From Gas to Walls
For the Cycle
°F Run No. 95
(α: B.T.U. / hr.sq.ft.°F)
200
180
160
140
120
100
80
60
40
20
T.D.C.
B.D.C.
T.D.C.
B.D.C.
T.D.C.
Intake
Compression
Expansion
Exhaust
0
45
90
135
180
225
270
315
360
Crank Angles

Figure 16.

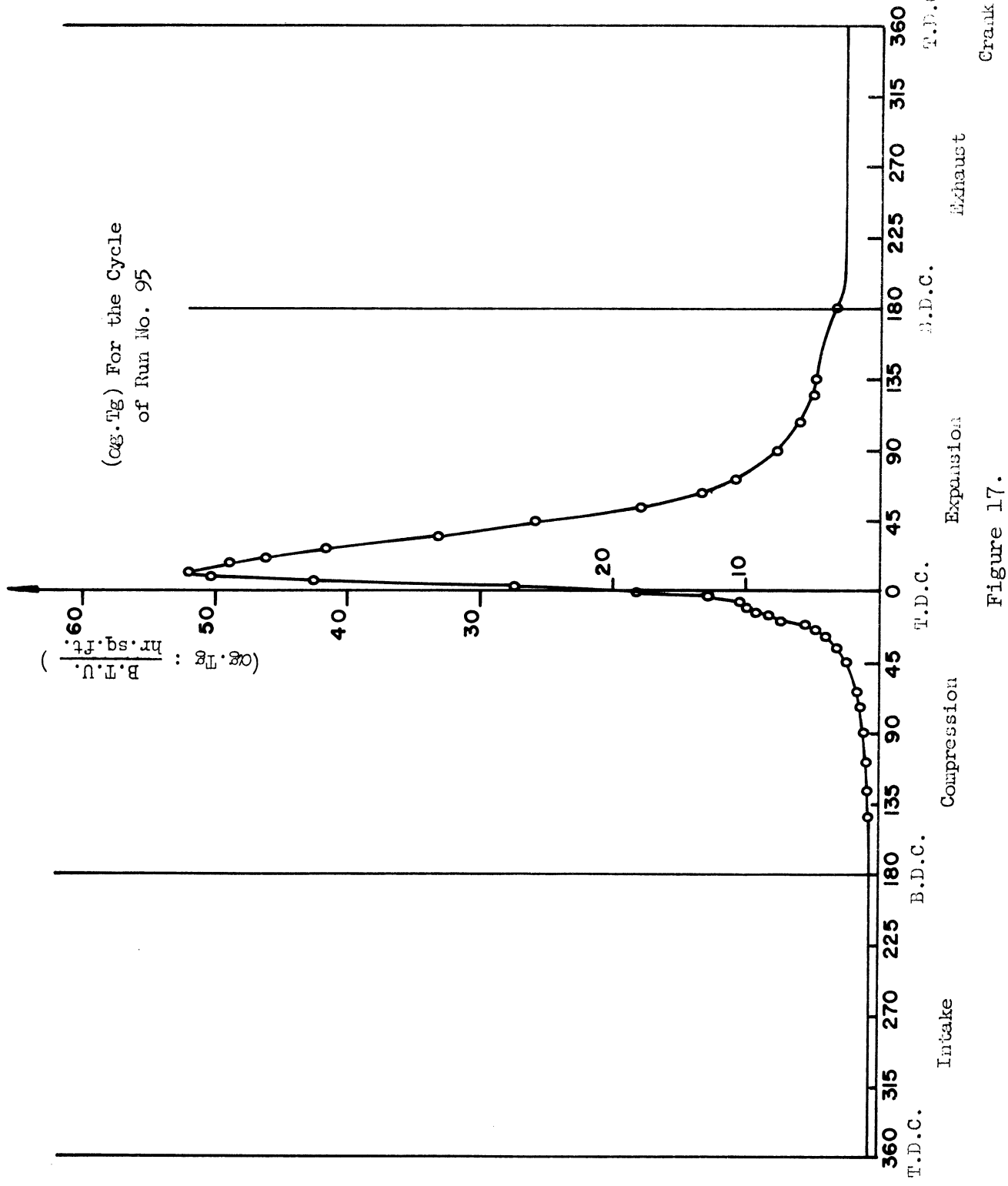
(αg.Tg) For the Cycle
of Run No. 95
(αg.Tg : B.T.U. / hr.sq.ft.)
60
50
40
30
20
10
0
45
90
135
180
225
270
315
360
T.D.C.
B.D.C.
T.D.C.
B.D.C.
T.D.C.
Intake
Compression
Expansion
Exhaust
Crank Angles

Figure 17.

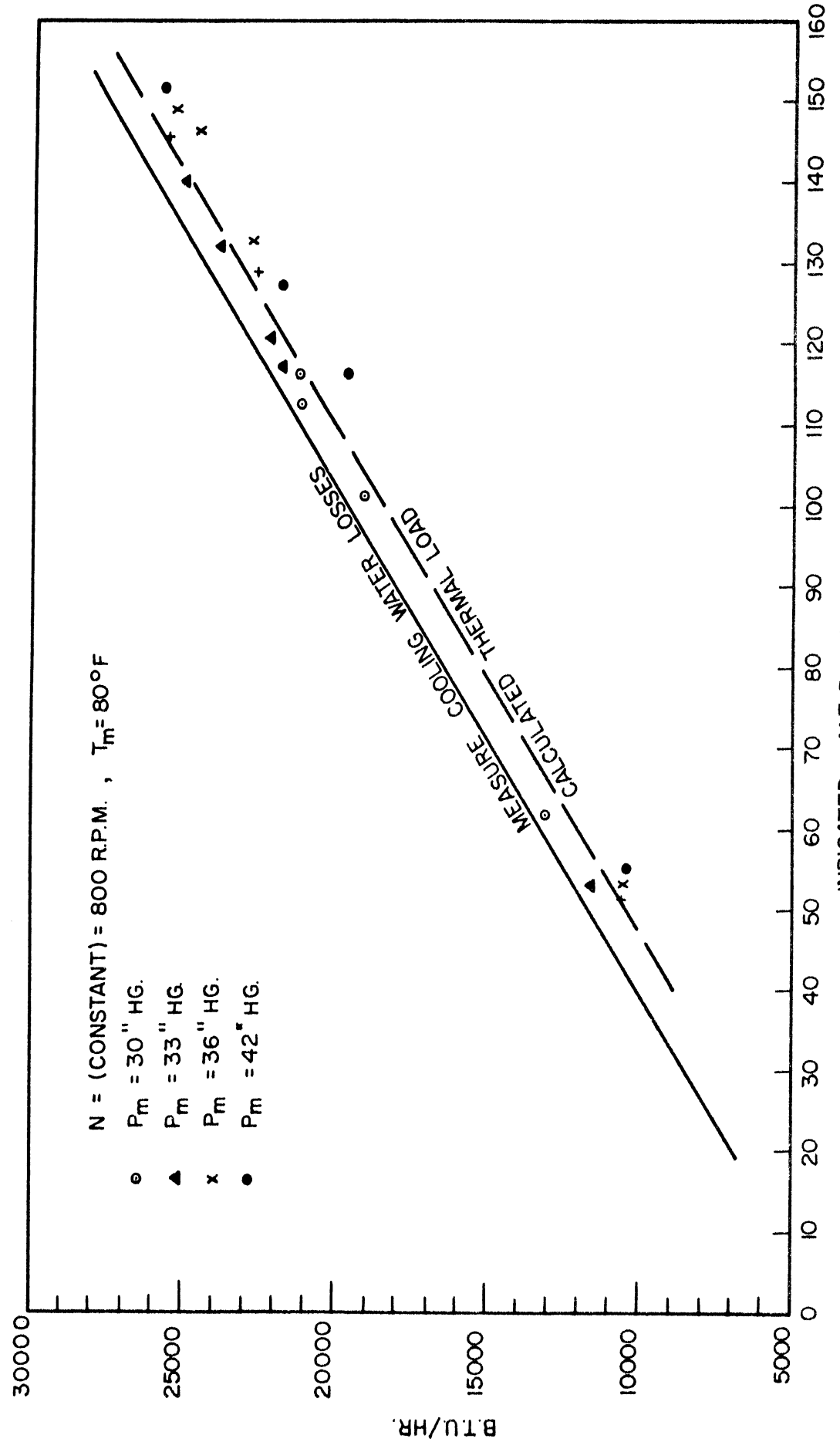

Figure 18. Comparison Between the Calculated Thermal Loads and Cooling Water Losses.

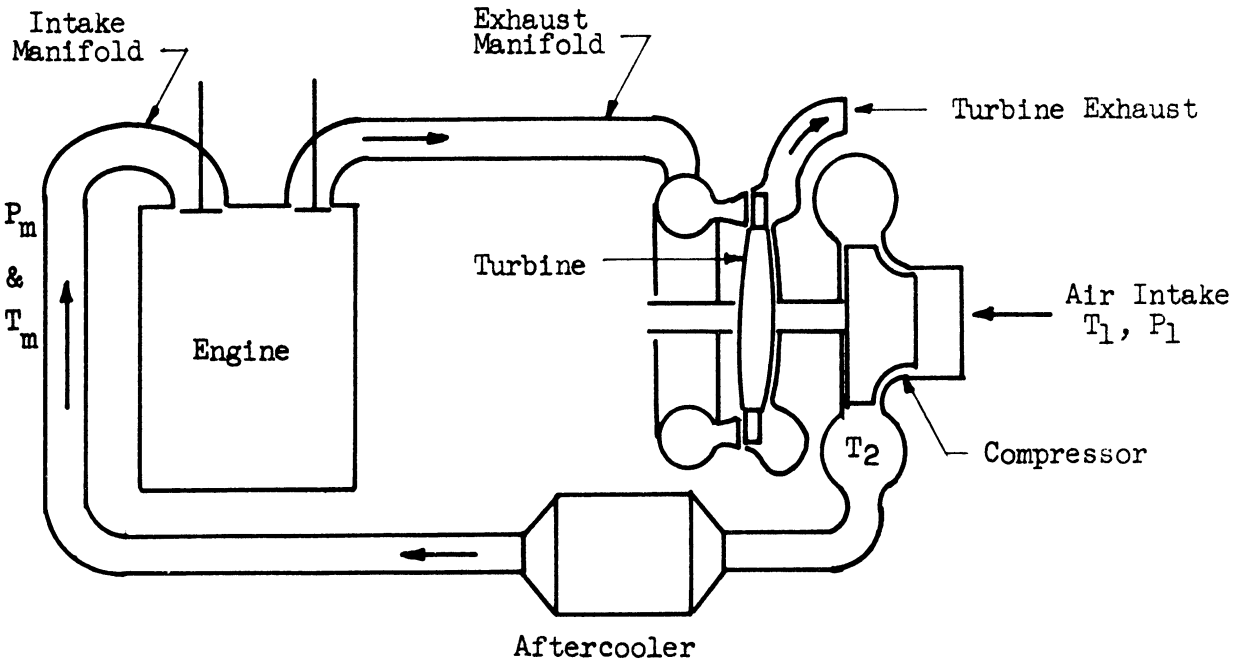

Figure 19. Diagram of Assumed Turbocharged C.I. Engine.

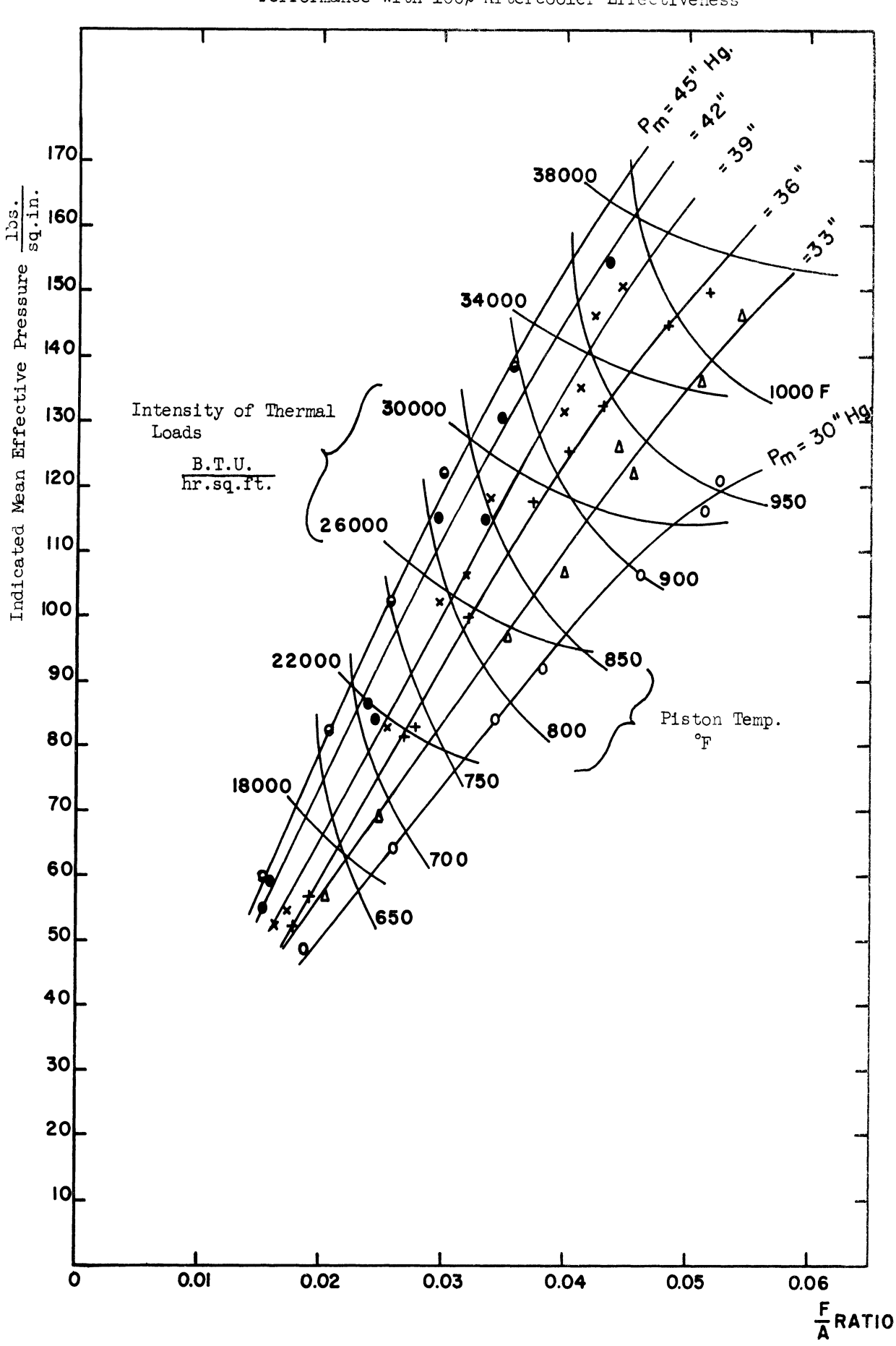
Performance With 100% Aftercooler Effectiveness
Indicated Mean Effective Pressure lbs./sq.in.
Pm = 45" Hg.
= 42"
= 39"
= 36"
= 33"
38000
34000
30000
26000
22000
18000
1000 F
950
900
850
800
750
700
650
Pm = 30" Hg.
Intensity of Thermal Loads
B.T.U./hr.sq.ft.
Piston Temp. °F
170
160
150
140
130
120
110
100
90
80
70
60
50
40
30
20
10
0
0.01
0.02
0.03
0.04
0.05
0.06
F/A RATIO

Figure 20.

Performance With 50% Aftercooler Effectiveness

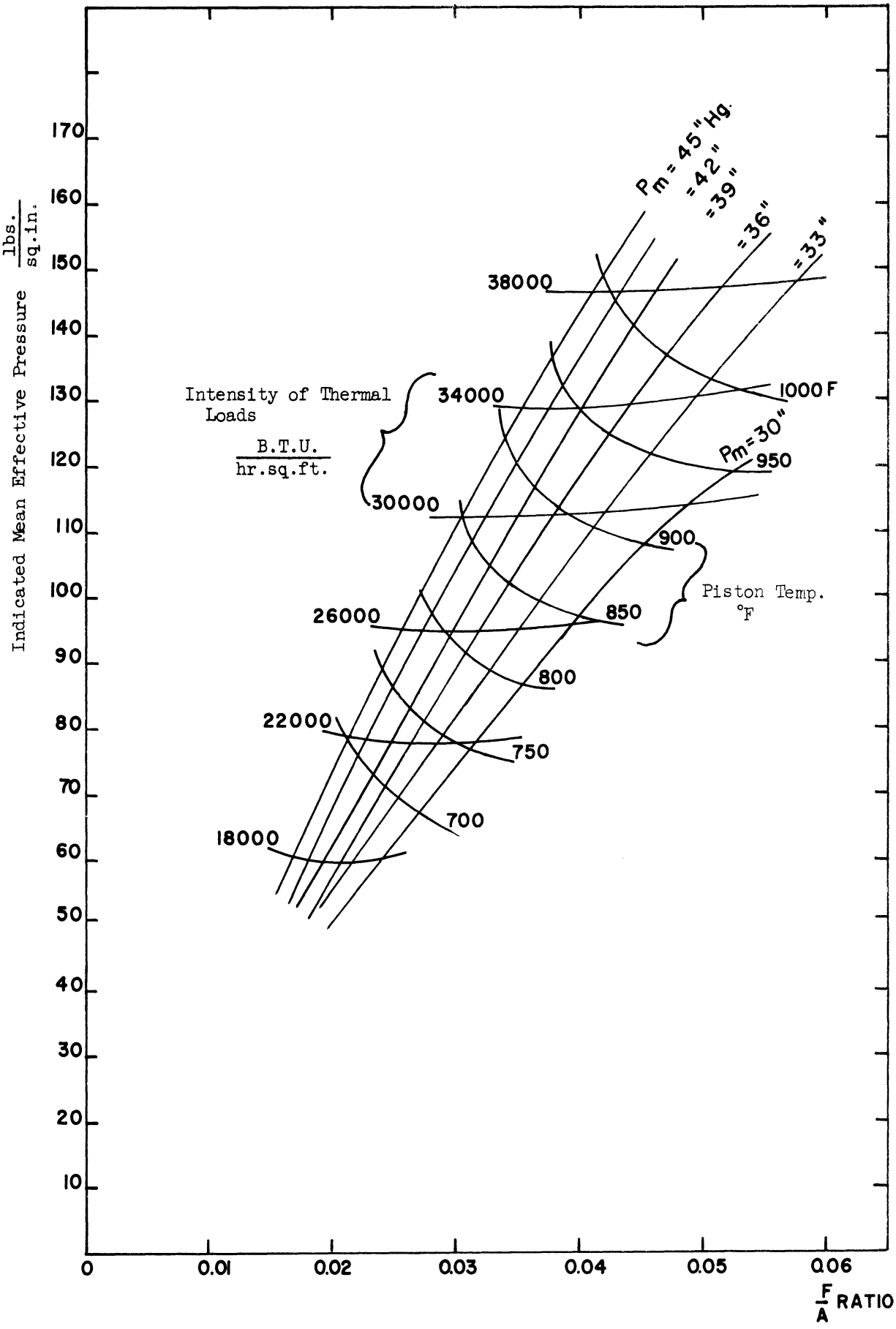

Figure 21.

Performance Without Aftercooling

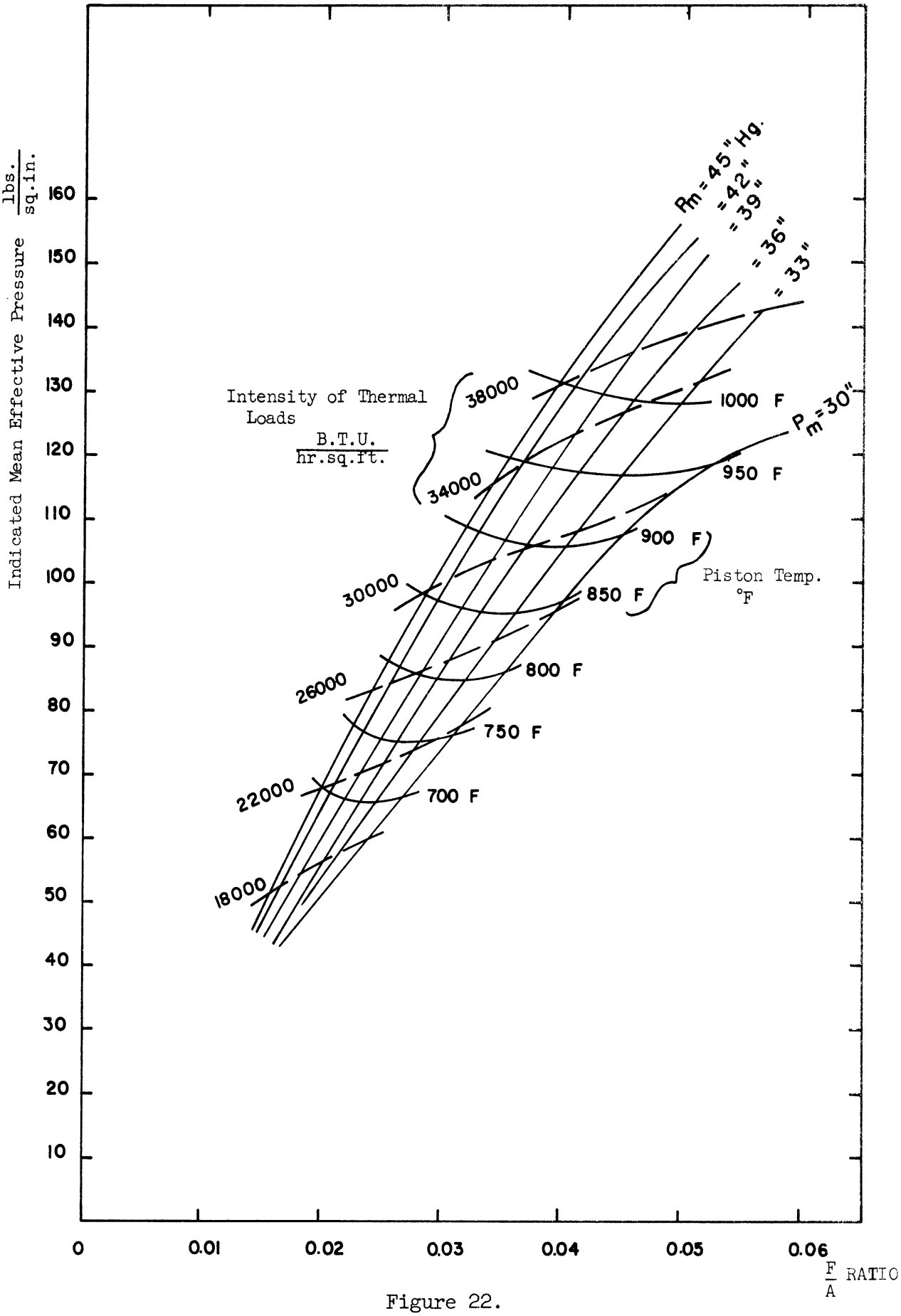

Figure 22.

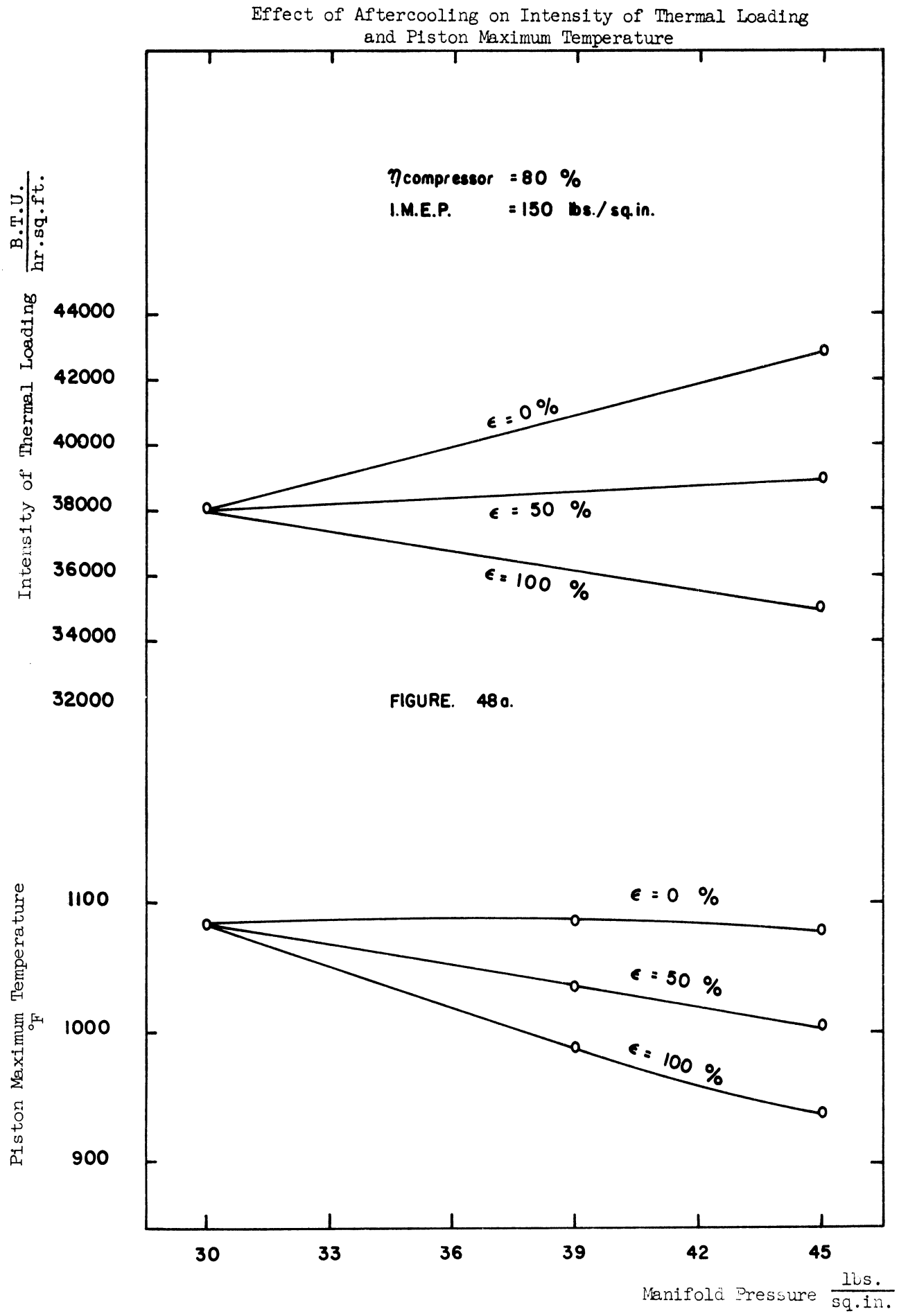
Effect of Aftercooling on Intensity of Thermal Loading
and Piston Maximum Temperature
ηcompressor = 80 %
I.M.E.P. = 150 lbs./sq.in.
Intensity of Thermal Loading B.T.U./hr.sq.ft.
44000
42000
40000
38000
36000
34000
32000
ε = 0 %
ε = 50 %
ε = 100 %
FIGURE. 48a.
Piston Maximum Temperature °F
1100
1000
900
ε = 0 %
ε = 50 %
ε = 100 %
30
33
36
39
42
45
Manifold Pressure lbs./sq.in.

Figure 23.

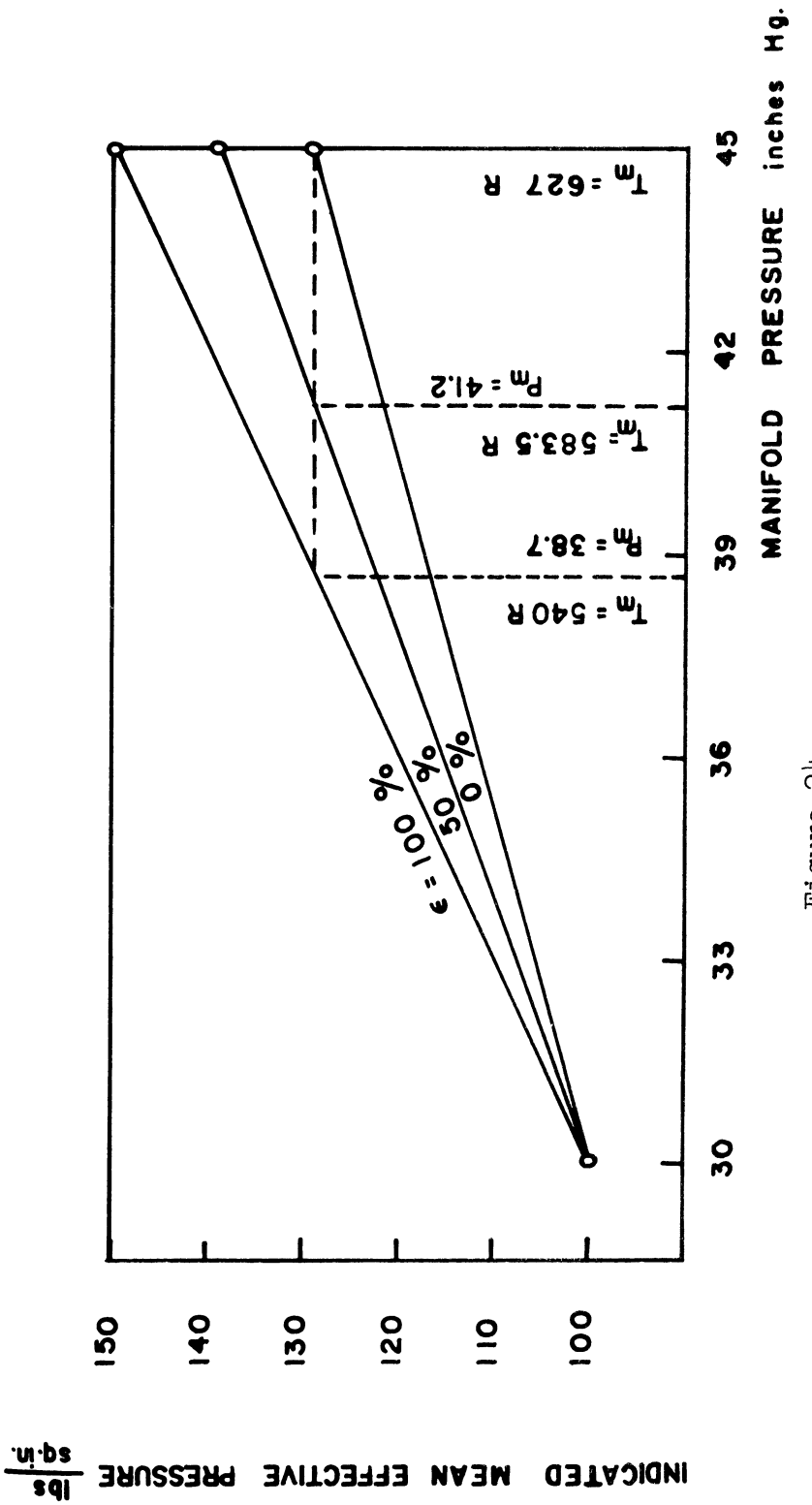
INDICATED MEAN EFFECTIVE PRESSURE lbs/sq.in.
150
140
130
120
110
100
30
33
36
39
42
45
MANIFOLD PRESSURE inches Hg.
ε = 100 %
50 %
0 %
Tm = 540 R
Rm = 38.7
Tm = 583.5 R
Pm = 41.2
Tm = 627 R

Figure 24.

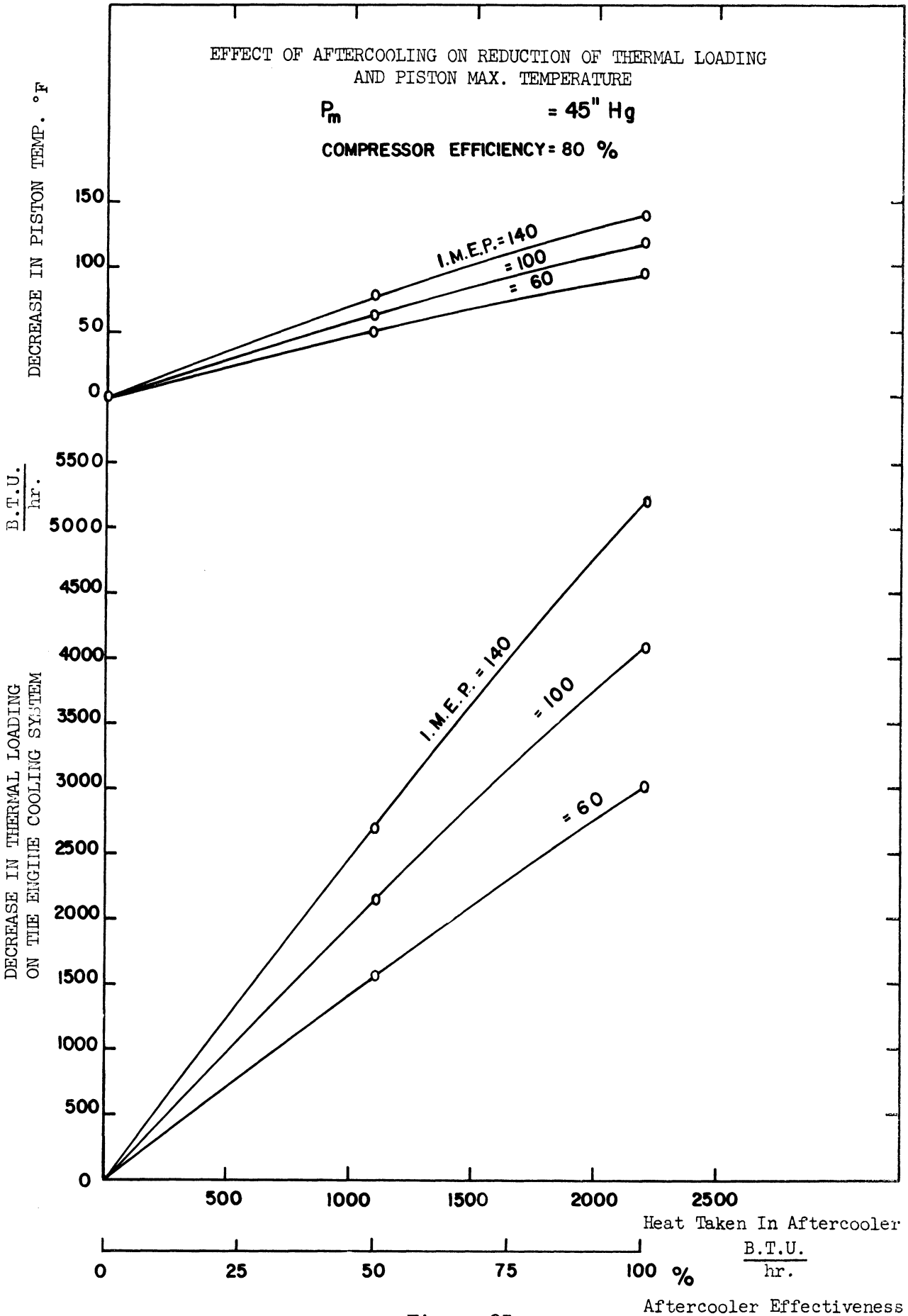
EFFECT OF AFTERCOOLING ON REDUCTION OF THERMAL LOADING
AND PISTON MAX. TEMPERATURE
P_m = 45" Hg
COMPRESSOR EFFICIENCY = 80 %
DECREASE IN PISTON TEMP. °F
150
100
50
0
I.M.E.P. = 140
= 100
= 60
B.T.U./hr.
DECREASE IN THERMAL LOADING ON THE ENGINE COOLING SYSTEM
5500
5000
4500
4000
3500
3000
2500
2000
1500
1000
500
0
I.M.E.P. = 140
= 100
= 60
500
1000
1500
2000
2500
Heat Taken In Aftercooler B.T.U./hr.
0
25
50
75
100 %
Aftercooler Effectiveness

Figure 25.